A

DISSERTATION REPORT

ON

DESIGN AND ANALYSIS OF HEXAGONAL, OCTAGONAL AND DECAGONAL PHOTONIC CRYSTAL FIBERS FOR VARIOUS OPTICAL PROPERTIES

is submitted as a partial fulfillment of the

MASTER OF TECHNOLOGY IN ELECTRONICS AND COMMUNICATION ENGINEERING

BY

AMRITVEER KAUR

(2015PEC5310)

UNDER THE GUIDANCE OF

Dr. RITU SHARMA

(Assistant Professor, ECE, MNIT, Jaipur)

DEPARTMENT OF ELECTRONICS AND COMMUNICATION ENGNEERING

MALAVIYA NATIONAL INSTITUTE OF TECHNOLOGY, JAIPUR

JUNE 2017

DEPARTMENT OF ELECTRONICS AND COMMUNICATION ENGINEERING

MALAVIYA NATIONAL INSTITUTE OF TECHNOLOGY

JAIPUR (RAJASTHAN)-302017

CERTIFICATE

This is to certify that the dissertation report entitled "**DESIGN AND ANALYSIS OF HEXAGONAL, OCTAGONAL AND DECAGONAL PHOTONIC CRYSTAL FIBERS FOR VARIOUS OPTICAL PROPERTIES"** submitted by **AMRITVEER KAUR**(2015PEC5310),in partial fulfilment of Degree **Master of technology** in **Electronics and Communication Engineering during** academic year 2016-2017. To best of my knowledge and belief that this work has not been submitted elsewhere for the award of any other degree.

The work carried out by her has been found satisfactory under my guidance and supervision in the department and is approved for submission**.**

Date:

Place:

Dr. Ritu Sharma

Assistant Professor

Department of electronics and communication

MNIT Jaipur

DEPARTMENT OF ELECTRONICS AND COMMUNICATION ENGINEERING

MALAVIYA NATIONAL INSTITUTE OF TECHNOLOGY

JAIPUR (RAJASTHAN)-302017

DECLARATION

This is to certify that the dissertation report entitled "**DESIGN AND ANALYSIS OF HEXAGONAL, OCTAGONAL AND DECAGONAL PHOTONIC CRYSTAL FIBERS FOR VARIOUS OPTICAL PROPERTIES"**being submitted by me in partial fulfilment of degree of **Master of Technology** in **Electronics & communications** during**2016-2017** in a research work carried out by me under supervision of **Dr. Ritu Sharma**, and content of this dissertation work in full or in parts have not been submitted to any other institute or university for award of any degree or diploma. I also certify that no part of this dissertation work has been copied or borrowed from anywhere else. In case any type of plagiarism is found out. I will be solely and completely responsible for it.

Place: **AMRITVEER KAUR**

Date: MTech (ECE)

2015PEC5310

MNIT Jaipur

Acknowledgement

This Dissertation report on "**DESIGN AND ANALYSIS OF HEXAGONAL, OCTAGONAL AND DECAGONAL PHOTONIC CRYSTAL FIBERS FOR VARIOUS OPTICAL PROPERTIES"** is carried out under the valuable guidance of supervisor Dr. Ritu Sharma (Assistant Professor, ECE, MNIT, Jaipur).

It is my privilege to express my deep sense of gratitude to her for her great efforts, ever helping attitude, critical and valuable comments and constant inspiration with akeen interest in making this dissertation report.

I am highly thankful to all faculty members of Electronics and Communication department for having their direct and indirect co-operation.

Finally, I gratefully acknowledge my parents and all my friends for their support and co-operation

TABLE OF CONTENT

LIST OF FIGURES

LIST OF TABLES

Abstract

During this MTech work, Attention has been focused on understanding and analyzing the modal behavior of Photonic Crystal Fibers. PCFs are fibers with complex dielectric topology and offer a number of novel possibilities, compared to standard Silica-based conventional optical properties.

The thesis focused on designing, simulating and analyzing the results of various designs of PCFs for their optical properties. The three geometries Hexagonal, Octagonal and Decagonal have been designed in order to compare its optical properties like Chromatic dispersion, Effective mode area, nonlinear coefficient and birefringence. All the simulations have been carried out on COMSOL Multiphysics 5.1 using Wave Optics Module. All the proposed structures are designed with doped Silica having refractive index 1.45. The results have been compared by varying different design parameters like air hole arrangements, pitch size, the diameter of air holes and shape of air holes of a structure.

Chapter 1

INTRODUCTION

Nowadays, the telecommunication industry relied on data transmission over optical fibers. It is the backbone of the information society as a huge amount of information is distributed through the network of fibers. The photonic crystal fiber presents a diversity of new and improved features over the conventional fibers. PCFs can be made using asingle type of glass, in contrast to conventional technology. In PCFs, light guidance can be achieved by introducing an air holes arrangement around the core and this arrangement of air holes run along the whole length of the fiber. In recent years, the optical fibers find extensive use within areas such as telecommunication, sensor technology, spectroscopy and medicine.

The final aim of this research work is to design, analyze and optimize the PCF parameters to achieve excellent properties. The ultimate goal of the research presented in this thesis is to propose some new design which could be fabricated and experimentally validate some pre-determined optical properties.

1.1 Basic concepts

1.1.1Conventional Optical Fibres

Conventional optical fibers guide light through total internal reflection (TIR). When light is incident on a boundary between two materials of different refractive indices, some light is reflected and some is refracted. At the angle greater than the critical angle all the light is reflected back into the material. Optical fibers in their simplest form achieve guidance through TIR by consisting of two regions: a high-index core and a cladding region of slightly lower refractive index enabling TIR along their length. The basic material used for the core and cladding is fused silica with different dopants. Long haul communications fibers consist of a germanium-doped core and pure silica cladding. The germanium doping gives a slightly higher refractive index than that of pure silica. Other dopants which raise the refractive index of silica are Aluminium, Phosphorus and Nitrogen, whereas Fluorine and Boron lower the

refractive index. The index-lowering dopants can be used to form low index claddings around a core formed from pure silica.

1.1.1(a) Guidance mechanism

The basic phenomenon of total internal reflection is introduced in terms of theplane wave rather than rays. Figure 1.1 depicts the infinitely long step-index fiber with circular cross section (radius ρ). The light propagating along the axis of the fiber (the z-axis) has a free-space wavelength λ, corresponding to a free-space wave number k_0(k_0= 2π/λ) and angular frequency $\omega = ck_0$(with c the velocity of light in a vacuum). Any electromagnetic radiation propagating along the fibre can be decomposed into plane waves through Fourier decomposition. In particular any field propagating along the z-axis can be decomposed as a superposition of fields that vary as exp($i(\beta z-\omega t)$) in both the cladding and the core. The quantity β is called the propagation constant. Thus light propagating in the core or the cladding can be consider as a superposition of plane waves with different wave vectors, with longitudinal components β and radial component (or perpendicular wave number)$k_\perp$(Figure1.1).

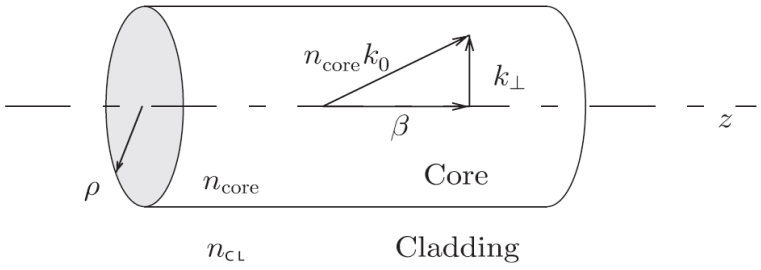

Figure 1.1: Conventional Step index fiber

In the corresponding ray picture, the wave vector of components β and $k_\perp$indicates the direction of the ray. In each medium, core or cladding, the refractive index determines the norm of each wave vector,$n_{core}k_0$and $n_{CL}k_0$, respectively. By the definition of the norm, we must have

$$k_\perp^2+\beta^2=n^2k_0^2 \quad (1)$$

Where n is the local refractive index (equal to n_{core}or to n_{CL}). While in order to have light propagating along z, β needs to be real rather than purely imaginary,$k_\perp$can be either real or imaginary. In what follows, it is assumed (without restricting the generality of the statements) that β is positive if $k_\perp$is real, the associated plane waves

are ‘propagative’ along the radial direction *r* and so light can radiate away from the fibre’s axis. If $k_{\cdot}$is imaginary, the plane waves are evanescent away from the fibre origin, and energy cannot propagate away from the fibre’s axis. It is clear that if light is allowed to propagate away from the fibre axis ($k_{\cdot}$real in the cladding), all energy will eventually be lost from the core: to guide light along the fibre $k_{\cdot}$must thus be imaginary in the cladding. From Eq. (1) the guided waves must thus have $\beta > n_{CL}k_0$. In the core on the other hand, $k_{\cdot}$can be either real or imaginary. However, it can be shown that in the most usual case where both the core and cladding are transparent dielectrics, no solutions with imaginary $k_{\cdot}$in the core exist, and thus propagative fields have $\beta < n_{core}k_0$. The *effective index* $n_{eff}$of fields with propagation constant β, defined as $n_{eff} \equiv \beta/k_0$. If $n_{CL} < n_{eff} < n_{core}$, light can propagate in the core, but is radially evanescent in the cladding: the light is trapped in the core. If $n_{eff} < n_{CL}$ light can propagate in the cladding away from the core, and is thus lost.

1.1.2Photonic crystal fibers

In 1996, a new kind of optical fiber was reported which, instead of having a cladding region formed from one glass, had a cladding region comprising an array of microscopic air holes running along the fiber length. This became known as photonic crystal fiber (PCF) and is represented schematically in Figure 2

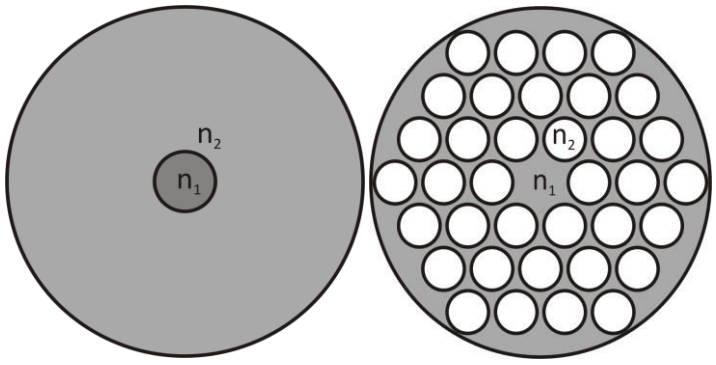

(a) (b)

Figure 1.2: Schematic representations of cross sections through (a) a conventional optical fiber and (b) a solid core photonic crystal fiber. In (a) the darker gray region representsthecore, consisting of a glass of slightly higher refractive index than that of the cladding region shown in a lighter gray. In (b) the white regions in the cladding represent an array of air holes run throughout the whole length of thefiber.

The array of air holes in the cladding gives PCFs significantly different guidance properties from conventional TIR guiding fibers. This is because the index contrast between the core (typically pure silica) and the cladding can be varied by altering the size of the cladding air holes, which changes the effective refractive index of the cladding region. Control of the effective refractive index allows significant engineering of fiber properties such as dispersion and nonlinearity.

PCFs are principally defined by three key parameters as shown in Figure 3, the centre to centre separation of the cladding inclusions (either air holes or doped glasses) Λ (pitch), the diameter of the cladding inclusions d, and the core diameter ρ defined as the shortest distance across the core between the closest spaced cladding inclusions.

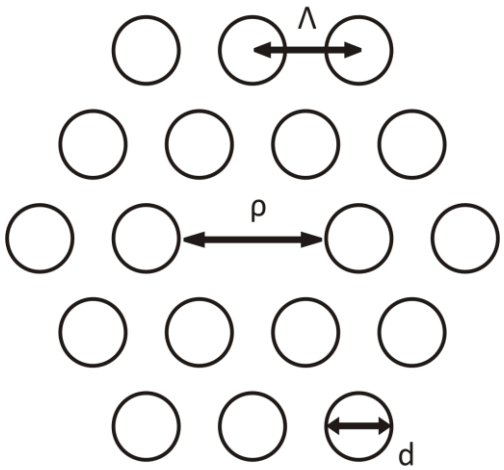

Figure 1.3: The key photonic crystal fiber parameters: Λ is the center to center separation of the cladding inclusions (pitch), d is the diameter of the cladding inclusions and ρ is the core diameter.

Photonic Crystal Fibers are divided into two categories on the basis of their guidance mechanism:

- high index guiding fibers
- low index guiding fibers.

1.1.2(a) High index guiding fibers

These are the fibers with a solid core or a core with a higher average index than the micro structured cladding. The light is confined in the core by exploiting the modified total internal reflection mechanism.

1.1.2(b) Low index guiding fibers

It is a hollow core fiber in which light is confined to the low index core. In this, the guiding mechanism is based on Photonic Band Gap (PBG) effect which makes impossible for particular frequency range to propagate in the micro structured cladding region.

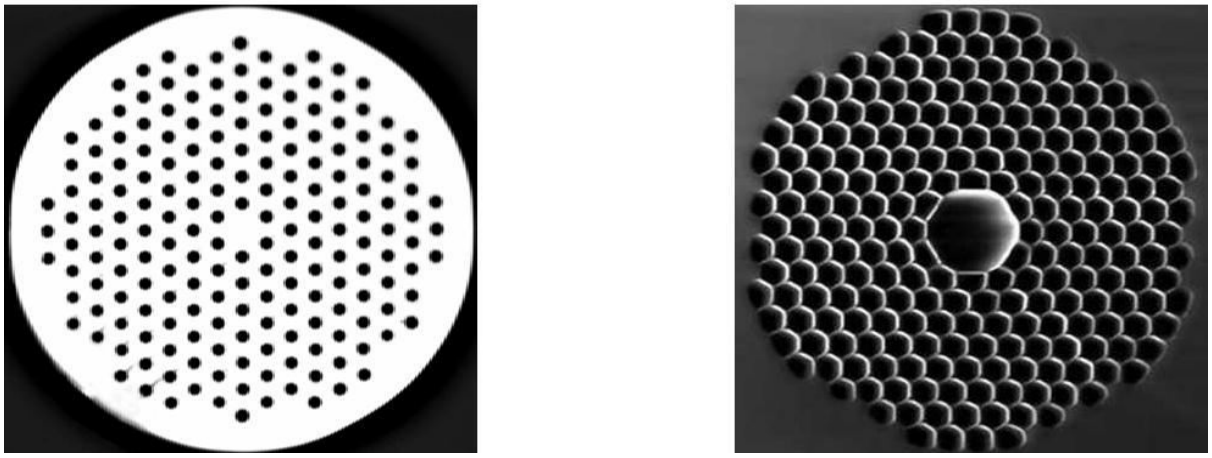

(a) **(b)**

Figure 1.4: Structure of (a) High index guiding fiber and (b) Low index guiding fiber

1.2 Basics equations

Propagation of light in PCFs is described by Maxwell's equations. For no free charge or current, the following equations become applicable

$$\nabla . D = 0 \qquad (1.2.1)$$

$$\nabla \times H = \frac{\partial D}{\partial t}$$

$$\nabla . B = 0$$

$$\nabla \times E = -\frac{\partial B}{\partial t} \qquad (1.2.2)$$

Restrict to linear low loss media with no frequency dependence of dielectric function such that the following equations become true

$$\varepsilon(\mathrm{r},\omega) = \varepsilon(\mathrm{r}) \in R$$

$$\mathrm{D(r)}=\varepsilon(r) \times \varepsilon o \times E(r) \qquad (1.2.3)$$

$$B = \mu o \times H$$

(1.2.4)

Inserting equation (1.2.3) into (1.2.1)

$$\nabla . \varepsilon(r) \times \epsilon o \times E(r,t) = 0$$

$$\nabla \times H(r,t) = \varepsilon(r) \times \varepsilon o \times \frac{\partial E(r,t)}{\partial t}$$

$$\nabla . \mu o . H(r,t) = 0$$

$$\nabla \times E(r,t) = -\mu o . \frac{\partial H(r,t)}{\partial t} \qquad (1.2.5)$$

Since Maxwell's equations are linear we can separate out the time dependence by expanding into a set of harmonic modes

$$H(r,t) = H(r) . e^{j\omega t}$$

$$E(r,t) = E(r) . e^{j\omega t} \qquad (1.2.6)$$

To obtain coupled equations we need the following ones

$$\nabla . \varepsilon(r) . E(r) = 0$$

$$\nabla \times H(r,t) = j\omega\varepsilon(r)\varepsilon o E(r)$$

$$\nabla . H(r) = 0$$

$$\nabla \times E(r) = j\omega . \mu o . H(r) \qquad (1.2.7)$$

Decoupling by dividing the dielectric function and taking curl yields

$$\nabla \times \left(\frac{1}{\varepsilon(r)} \nabla \times H(r)\right) = \left(\frac{\omega}{c}\right)^2 . H(r) \qquad (1.2.8)$$

For a given frequency, this equation completely determines the modes H(r) and the required transversality. There are many different methods to solveeigenvalue problem, but so far all methods rely on numerical calculations.

1.3 Properties of PCF

These are some properties of PCF which depends upon the geometrical arrangement of holes in the fiber cross-section, which are listed below:

1.3.1 Effective refractive index

The effective refractive index is a measure of the overall delay of a light beam in an optical component. In homogeneous transparent media, the refractive index *n* can be used to quantify the increase in the wave number (phase change per unit length) caused by the medium: the wave number is *n* times higher than it would be in a vacuum. The *effective refractive index n*eff has the analogous meaning for light propagation in a waveguide; the β value (phase constant) of the waveguide (for some wavelength) is the effective index times the vacuum wave number:

$$\beta = n_{eff} \frac{2\Pi}{\lambda} \tag{1.3.1}$$

1.3.2 Normalized frequency of PCF

The single modeness of the fiber can be verified by effective V parameter within telecom band. For PCFs, the formula used to calculate V parameter is given as:

$$V_{eff} = \frac{2\Pi\Lambda}{\lambda}\sqrt{n_{co} - n_{eff}} \tag{1.3.2}$$

Where, n_{co} is the refractive index of core material, n_{eff} is the effective refractive index of the cladding, Λ is pitch size and λ is wavelength. It is known that the condition for higher order mode cutoff is associated with $V_{eff} \leq \Pi$ at 1550nm.

1.3.3 Chromatic Dispersion

Basically, Dispersion is the time domain spreading and broadening of the transmission signal light pulses, as they travel through the fiber and results in error and loss of information. In PCFs, the Chromatic dispersion is a combination of material dispersion and waveguide dispersion. Material dispersion comes from a frequency-dependent response of a material to waves and Waveguide dispersion occurs when the speed of a wave in a waveguide or fiber depends on its frequency for geometric reasons. In any material, the refractive index depends on frequency. The chromatic dispersion D of a PCF is easily calculated from the effective index of the fundamental mode n_{eff}, using

$$D = -\frac{\lambda}{c}\frac{d^2 n_{eff}}{d\lambda^2} \quad (1.3.3)$$

Where *c* is the velocity of light in a vacuum.

1.3.4 Modal Birefringence

Refractive index sometimes depends on the polarization and on propagation direction of light. So the refractive index of the two fundamental modes (x and y mode) will not be same. Birefringence is the difference of effective index between these two fundamental modes. Birefringence can be calculated using the equation

$$\text{Birefringence} = \left| n_{eff}(xmode) - n_{eff}(ymode) \right| \quad (1.3.4)$$

1.3.5 Effective Modal Area

The effective mode area A_{eff}, is related to the effective area of the fiber core area which is computed using transverse electric or magnetic field vector of the whole cross-sectional area of the fiber. The effective area of the of the fiber core A_{eff} is defined as

$$A_{eff} = \frac{(\iint |E_t|^2 dxdy)^2}{\iint |E_t|^4 dxdy} \quad (1.3.5)$$

$$A_{eff} = \frac{(\iint |H_t|^2 dxdy)^2}{\iint |H_t|^4 dxdy} \quad (1.3.6)$$

Where E_t and H_t is the transverse electric field vector and magnetic field vector respectively and the integration is done through the whole cross sectional area of the fiber.

1.3.6 Non-linearity coefficient

Due to different scattering phenomenon, the intensity depends on refractive index in the medium which results in the occurrence of nonlinear effect in the optical fiber. The nonlinearity depends on the type of material and design of the fiber. The nonlinear coefficient, γ in $(\text{W.km})^{-1}$ is calculated by the following equation:

$$\gamma = \frac{n_2 \omega}{c A_{eff}} = \frac{n_2 2\Pi}{\lambda A_{eff}} \quad (1.3.7)$$

where n_2 is the nonlinear-index coefficient in the nonlinear part of the refractive index.

1.3.7 Confinement Loss

The presence of finite air holes in the core region causes leakage of optical mode from inner core region to outer air holes is unavoidable which results in confinement losses. The confinement loss of the fundamental mode can be calculated from the imaginary part of the complex effective refractive index neff, using,

$$\text{Confinement loss} = 8.686 \times 10^{6} \times k_0 \times \text{Im}(n_{eff}) \quad \text{(dB/m)} \quad (1.3.8)$$

CHAPTER 2

Literature survey

The first practical existence of PCF was introduced in 1996 as a low loss waveguide. Due to novel optical properties of PCFs, this area of photonics has become an active field of research over the recent years. The tremendous growth in data traffic in telecommunication industry has increased the demand for intensive bandwidth. To improve its capability this field is one of the methods to meet this requirement of the high data rate.

The photonic crystal fiber presents a diversity of new and improved features over the conventional fibers. PCFs are having special properties and capabilities due to its geometric structure which leads to its outstanding potential for sensing applications. The waveguide properties like waveguide dispersion, birefringence, nonlinearity and polarization etc of the photonic crystal fibers depend on arrangement and shape of air holes which run through the whole length of the fiber. PCFs possess numerous properties in terms of transmission characteristics such as dispersion compensation, high nonlinearity, flat dispersion, large mode area and high birefringence. [9]

The chromatic dispersion can be made more flattened over a wide frequency range for large bandwidth applications and it can also be made negative in order to use them a dispersion compensation fibers. In 2016, a geometry with circular lattice has reported ultra-flattened average dispersion of -124.0 ps/(nm-km) with a dispersion variation of $\pm$0.1252 ps/(nm-km) over the wavelength range of 1350 to 1700 nm at very low confinement loss of 10^{-6}dB/km. [18]

With some certain structural arrangement of geometry, the light can be made more bounded to the core portion which in turn minimizes its effective area and increases nonlinearity. The highly nonlinear fibers may be applicable for certain applications like optical parametric amplifier and oscillator, optical code division multiplexers, multiwavelength lasers.

The asymmetric microstructure design around the fiber core may lead to achieving higher birefringence. The highly birefringent fibers can be used in applications like fiber optic sensing and coherent optical communications. The asymmetricity near the

core can be created by using an asymmetric arrangement of air holes around the core or by using variable air hole sizes or by non-circular air holes.

Till now various designs for pressure sensors have been proposed for its sensitivity with a solid core, hollow core, dual core or with various geometries. The hexagonal structure with two elliptical hollow channels stressed at major axis in the cladding region reported a high birefringence of 1.2×10^{-2}. [4]. The squeezed hexagonal PCF with two missing air holes in the first ring reported birefringence of 1.45×10^{-2} with nonlinear coefficient of 16.54 $W^{-1}km^{-1}$[2]. The octagonal PCF with variable diameter of holes in various rings and elliptical core reported birefringence of 2.04×10^{-2} and higher nonlinear coefficient of $33W^{-1}km^{-1}$at 1.55μm. [1]

CHAPTER 3

COMSOL Multiphysics

COMSOL Multiphysicsis a software platform used for modeling, solving and analyzing various engineering problems on the basis of Partial Differential Equations (PDEs) using Finite element method (FEM).

There are several modules are available in multiphysics which is categories according to their application areas. For this research, Wave Optics Module has been used specifically. The wave optics module can model high-frequency electromagnetic wave simulations in either frequency domain or time domain for optical structures.

3.1 Simulation methodology

For simulation in COMSOL, adaptive meshing and various numerical techniques for error control are used for finite element analysis.This study has been carried out over the frequency range of 700 nm to 2000 nm. The Maxwell equations are solved using FEM, in which Eigenvalue problem is solved to calculate the propagation of electric vector for full vector analysis of fiber. This analysis is done for each triangular region of mesh to obtain the effective refractive index of the PCF. The scattering boundary conditions are applied to the cladding region of the PCF in order to lock the reflection caused by leaky modes into the core region of the fiber.

3.2 Design methodology

The three different types of geometries have been designed on COMSOL MultiPhysics Software Version 5.1:

- Hexagonal
- Octagonal
- Decagonal

The diameter of air the holes and pitch size, ∧ (distance between adjacent holes) are the basic design parameters. Each geometry consists of an isosceles triangle with the vertex angle A. All the three geometries are having different vertex angles. The pitch size is taken as the length of the identical sides of the triangle. The length of the side opposite to the vertex angle is calculated as 2*p*sin(A). This isosceles triangle is a basic repetitive unit of each geometry.

Hexagonal

In this geometry, the numbers of air holes around central core (in the first ring) are 6 and the vertex angle of the isosceles triangle is60^0.

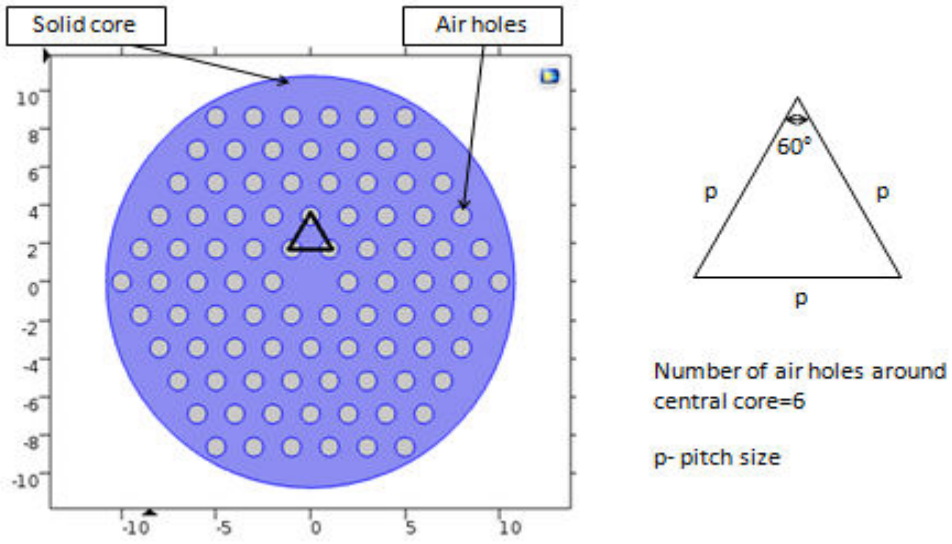

Figure 3.1: Snapshot of PCF with Hexagonal layout

Octagonal

In this geometry, the numbers of air holes around central core (in the first ring) are 8 and the vertex angle of the isosceles triangle is45^0.

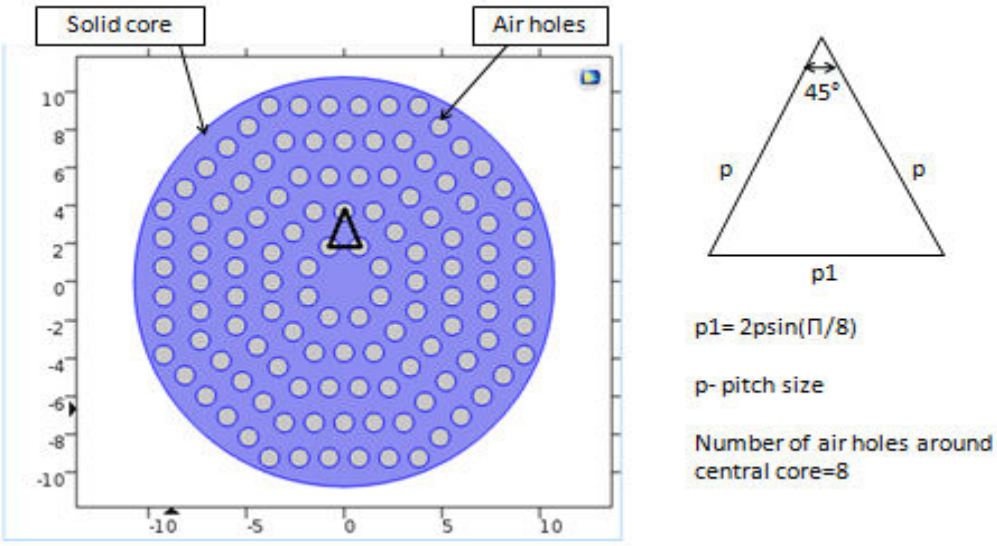

Figure 3.2: Snapshot of PCF with Octagonal layout

Decagonal

In this geometry, the numbers of air holes around central core are 10 and the vertex angle of the isosceles triangle is 36^0.

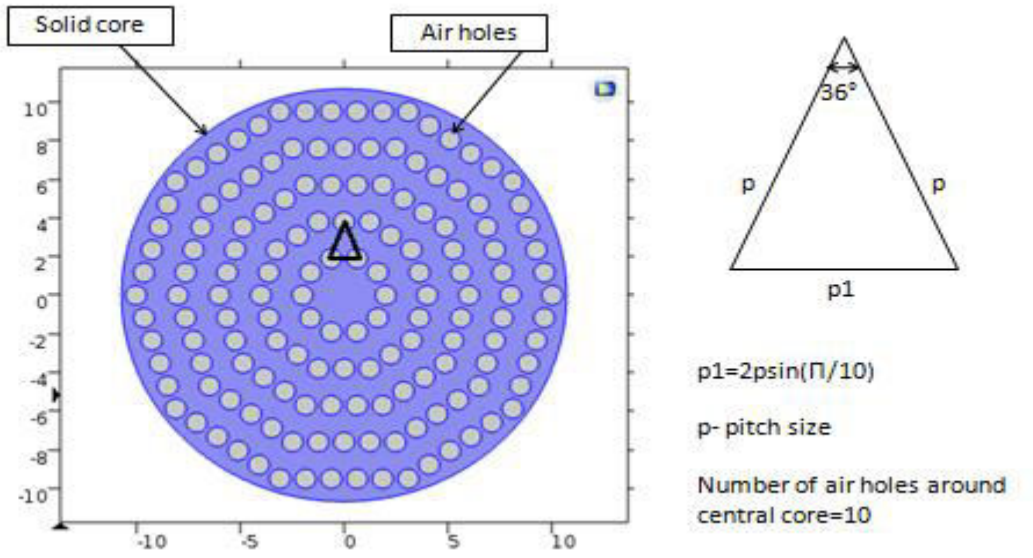

Figure 3.3: Snapshot of PCF with Decagonal layout

3.3 Steps involved in the design of PCF using COMSOL Multiphysics

COMSOL Multiphysics Software version 5.0 has a 2-D modal analysis used for PCF design using wave optics module.

Steps involved:

- **Defining parameters**: The parameters required for designing geometry like pitch size, hole diameter and for study analysis like refractive index, operating wavelength are defined.
- **Geometry Modelling**: Solid geometry is formed by using inbuilt primitive geometries like circle, ellipse, polygons etc and by using transform functions like an array, rotate, mirror image etc.
- **Defining material**: Material can be added from the material library or can be defined by the user for particular domains of the geometry.
- **Physics settings**: For this project, I have used wave optics module. Go to Add Physics>Optics>Wave Optics>Electromagnetic Waves, Frequency Domain (ewfd). Scattering boundary conditions are applied around cladding.
- **Generating Mesh**: Physics controlled mesh is used with normal element size.

- **Study and computing the solution:** Go to Add Study> Modal Analysis. Reset the mode analysis frequency and the refractive index of the core around which modes have to search. Parameterized sweep is applied to getting results at a different wavelength and then select Compute.
- **Post processing and visualization:**

  Results: Results are plotted for the effective refractive index, Electric field etc on 1D, 2D and 3D graphs accordingly.

  Export: Data and Plots are exported to Excel sheets for further calculations of dispersion.

CHAPTER 4

Basic designs of PCFs

The three basic designs of all three geometries Hexagonal, Octagonal and Decagonal which are explained earlier in chapter 3 has been designed with circular air holes. The various plots have been plotted to analyze the characteristics of Photonic crystal fiber for different structural geometries by varying its parameters. These are:

- Effective refractive index v/s wavelength
- Chromatic dispersion v/s wavelength
- Effective Area v/s wavelength

Parameters used:

- Pitch size=1 μm, 1.5 μm, 2 μm
- Diameter of hole to pitch ratio=0.3, 0.4, 0.5, 0.6
- Operating wavelength=1.55μm
- Refractive index of material used=1.45 (Doped Silica)
- Number of rings of air holes=5

Mode profile of a fundamental mode is given below, showing the confinement of the mode to the center of the PCF in all three geometries. The hexagonal shows six lobes in its mode profile, similarly octagonal shows eight and decagonal shows ten lobes. Decagonal shows more confined light.

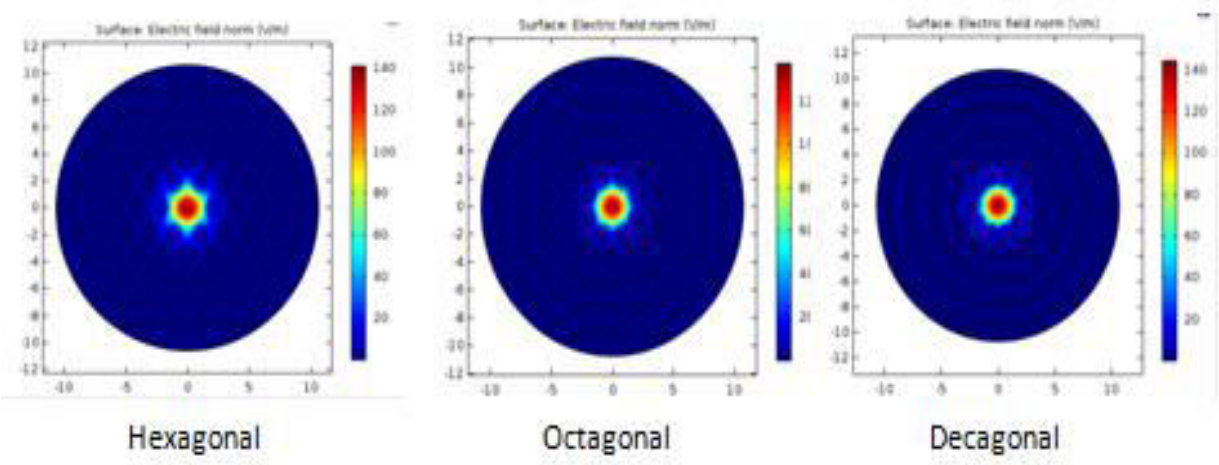

Figure 4.1: Power confinement patterns of all three geometries

4.1 Effective refractive index

The plot in figure 4.1represents the variation of effective refractive index with wavelength at constant values of the diameter of holes=0.5µm, pitch size=2µm and Number of rings=5.As geometry shifted to higher order polygon, the relative air fraction increases, hence effective refractive index decreases relatively.

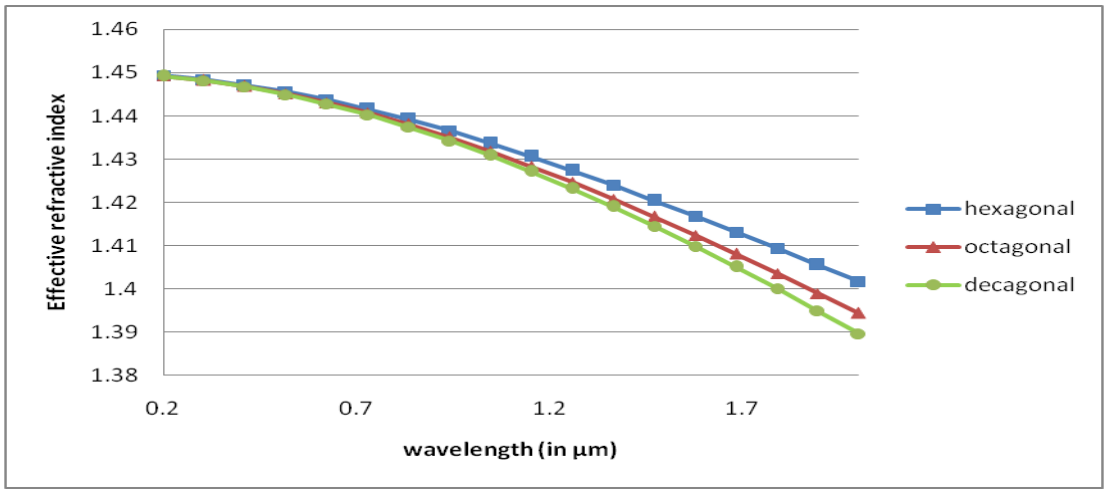

Figure 4.2: Plot of Effective Refractive index v/s Wavelength for three geometries with pitch length=2µm and air fraction, d/p=0.5

It is observed in Figure 4.2 that the value of effective refractive index decreases as the wavelength is increased justifying the Equation $n_{eff=}$ k/λ. The slope of curve is more for decagonal layout as it has more number of air holes surrounding the core and thus confines more light in the core.

4.2 Chromatic Dispersion

The Chromatic dispersion is basically a combination of waveguide dispersionDg and material dispersionDm in Photonic Crystal Fibers which is given as

$$D\ (\lambda) = Dg\ (\lambda) + \Gamma Dm\ (\lambda) \qquad (4.1)$$

Where Γ is the confinement factor, which depends on the material of fiber is close to unity for Silica. Both the dispersions can be calculated by

$$D = -\frac{\lambda}{c}\frac{d^2(Re[n_{eff}])}{d\lambda^2} \qquad (4.2)$$

where Re $[n_{eff}]$ is the real part of effective refractive index, c is the velocity of light in vacuum and λ is wavelength. The Sellmeier formula is used to calculate the effective refractive index for material dispersion is given as:

$$n^2=1+\frac{B_1\lambda^2}{\lambda^2-C_1}+\frac{B_2\lambda^2}{\lambda^2-C_2}+\frac{B_3\lambda^2}{\lambda^2-C_3} \quad (4.3)$$

where λ is operating wavelength in μm and the Sellmeier coefficients for silica are:
B_1=0.69616630,B_2=0.40794260,B_3=0.89747940,
C_1=0.068404300μm²,C_2=0.11624140μm²,C_3=9.8961610μm².

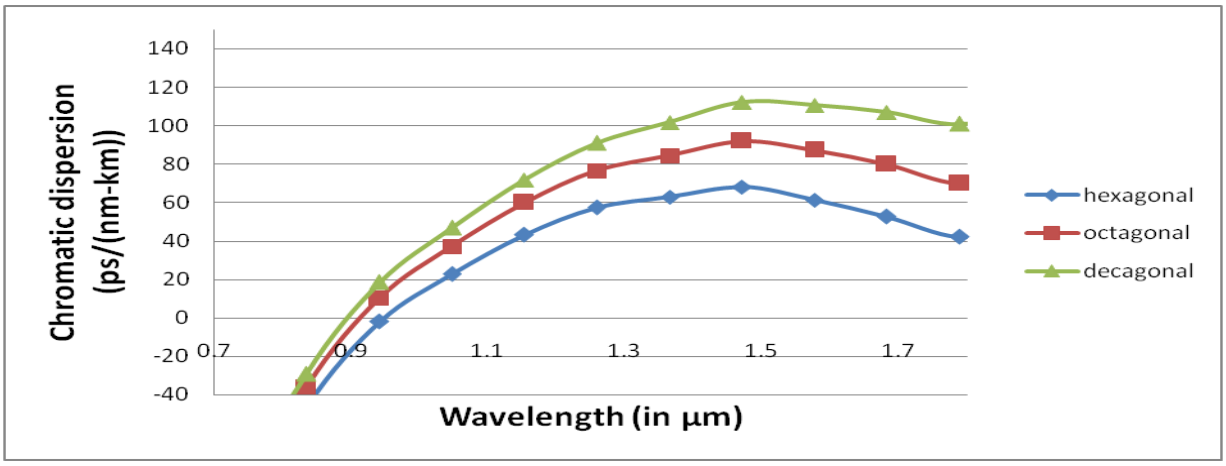

Figure 4.3: Comparative plot of Chromatic dispersion v/s wavelength for different geometries at pitch length=2μm and air filling fraction, d/p=0.5

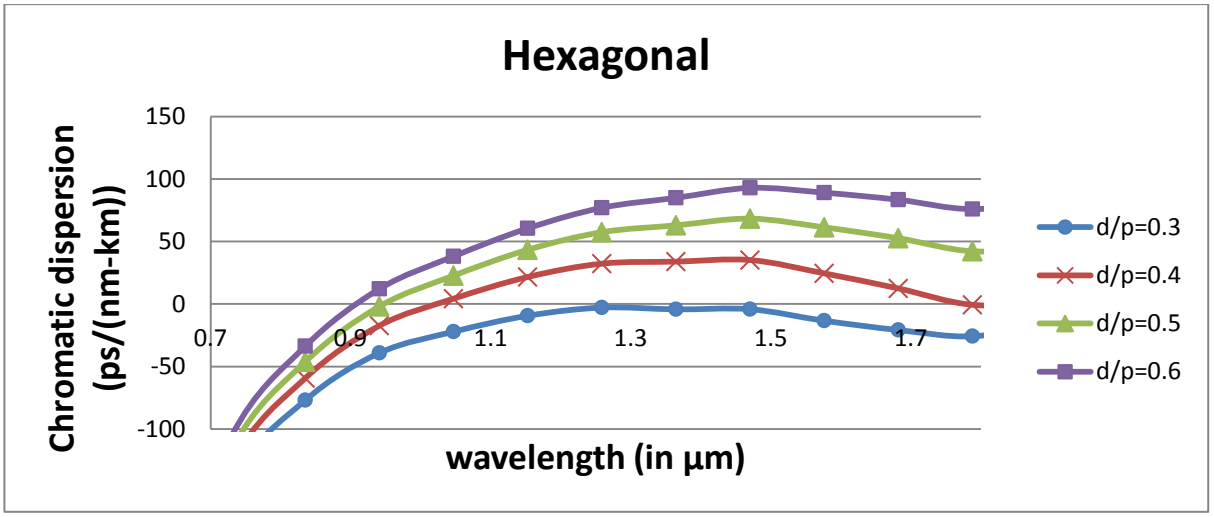

Figure 4.4: Chromatic dispersion v/s wavelength graph at pitch length=2μm for different air filling fractions (d/p) for Hexagonal Geometry

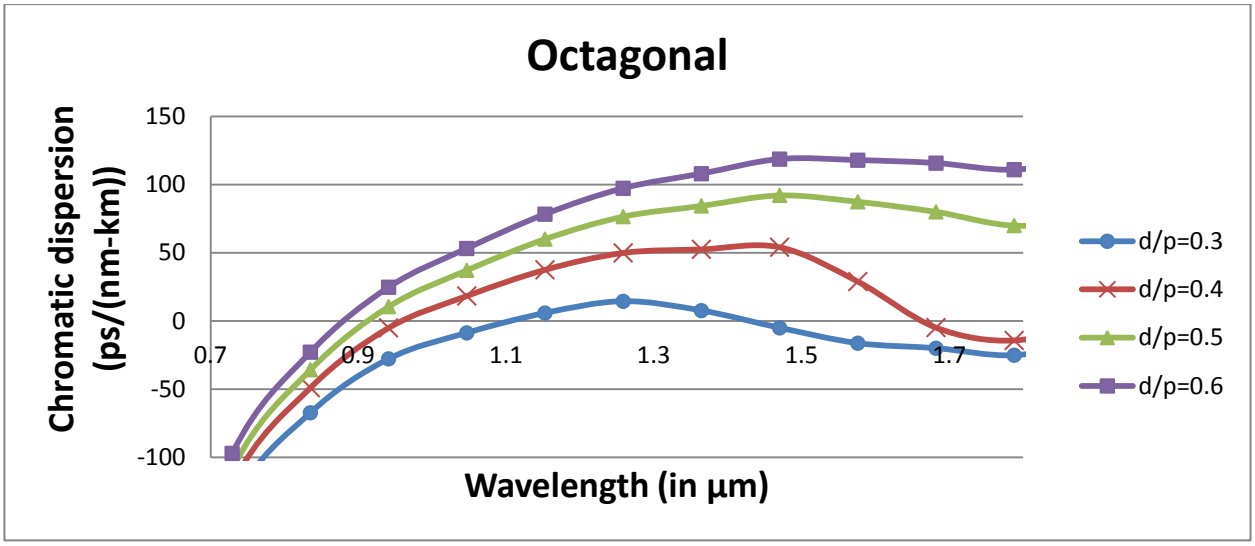

Figure 4.5: Chromatic dispersion v/s wavelength graph at pitch length=2µm for different air filling fractions (d/p) for Octagonal Geometry

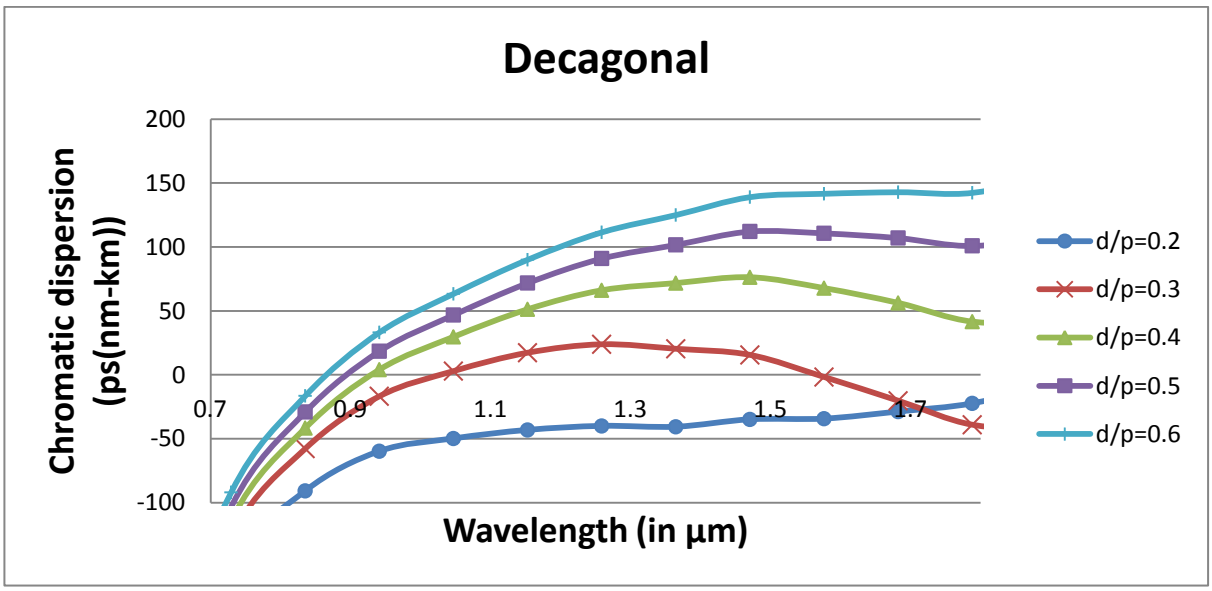

Figure 4.6: Chromatic dispersion v/s wavelength graph at pitch length=2µm for different air filling fractions (d/p) for Decagonal geometry

As diameter to pitch ratio increases, relative air fraction increases, zero dispersion wavelength get shifted to smaller wavelength, however, the magnitude of dispersion at operating wavelength increases.

Table 4.1: This table shows the zero dispersion wavelengths (in μm) of different geometries at different values of diameter to pitch ratio for same pitch size=2μm

	Hexagonal (in μm)	Octagonal (in μm)	Decagonal (in μm)
d/p=0.3	1.28	1.10	1.04
d/p=0.4	1.01	0.95	0.94
d/p=0.5	0.94	0.92	0.901
d/p=0.6	0.91	0.88	0.87

Table 4.2: shows the chromatic dispersion (in ps/(nm-km)) at λ=1.55μm for different geometries at different values of diameter to pitch ratio for same pitch size=2μm

	Hexagonal (ps/(nm-km))	Octagonal (ps/(nm-km))	Decagonal (ps/(nm-km))
d/p=0.3	-13.32	-16.30	-1.74
d/p=0.4	24.42	28.87	67.78
d/p=0.5	61.26	87.34	110.70
d/p=0.6	89.07	117.81	141.50

From Table 4.1 and Table 4.2 it can be seen that as the geometry gets shifted to higher order polygon or as the air filling fraction(d/p) increases, the dispersion curve shifts upward, Therefore the values of Chromatic dispersion at 1.55μm wavelength increases. Here, the decagonal structure at d/p=0.3 shows least dispersion magnitude. It can also be justified from equation 4.1 that for decagonal geometry the value of n_{eff} is less as compared to hexagonal or octagonal geometry hence less magnitude of dispersion.

4.3 Effective Mode Area

Effective mode area is calculated for all three geometries at different values of wavelength with adiameter(air hole) to pitch ratio as 0.5 and varying pitch size of 1μm, 1.5μmand 2μm.

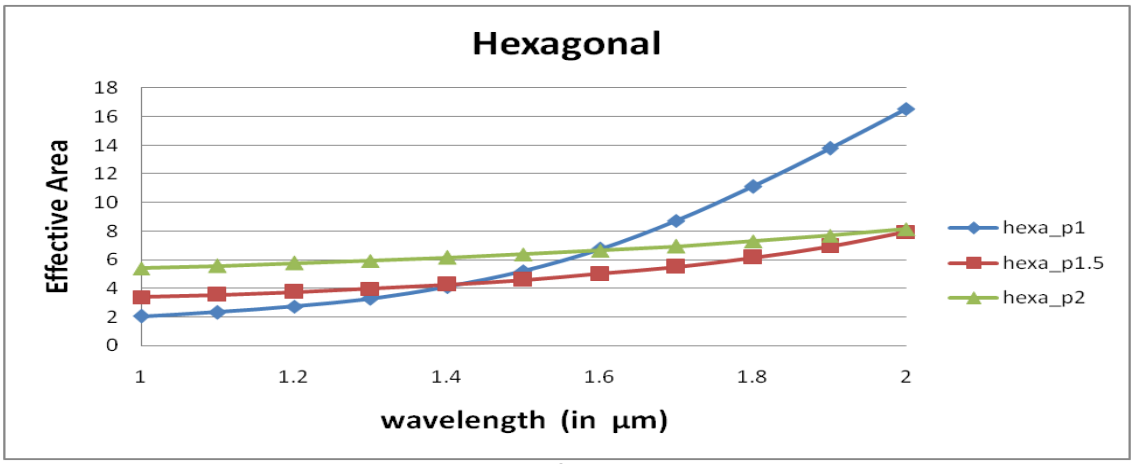

Figure 4.7: Effective Modal Area (in μm^2) v/s wavelength of hexagonal geometry with air filling fraction(d/p)=0.5 at different pitch sizes=1µm, 1.5µm, 2µm

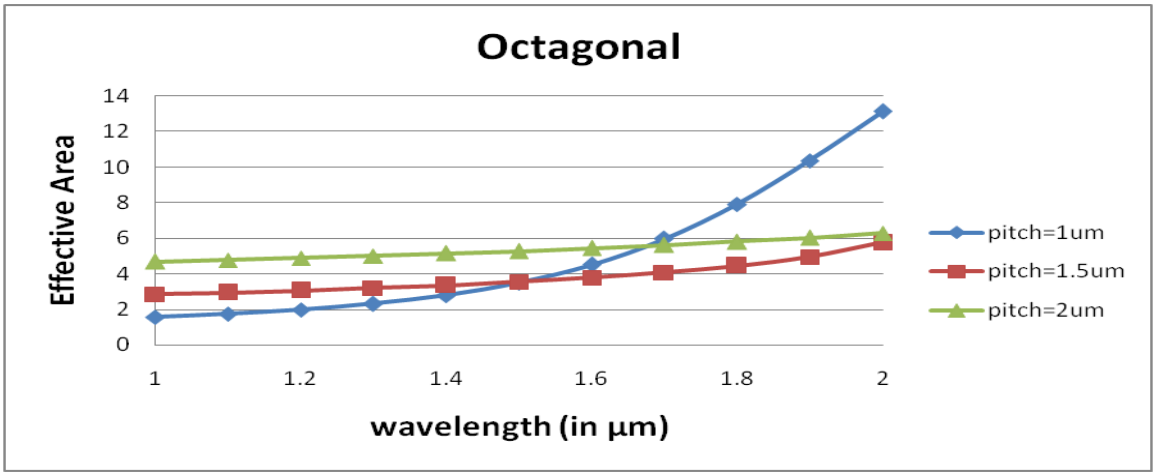

Figure 4.8: Effective Modal Area (in μm^2) v/s wavelength of Decagonal geometry with air filling fraction(d/p)=0.5 at different pitch sizes=1µm, 1.5µm, 2µm

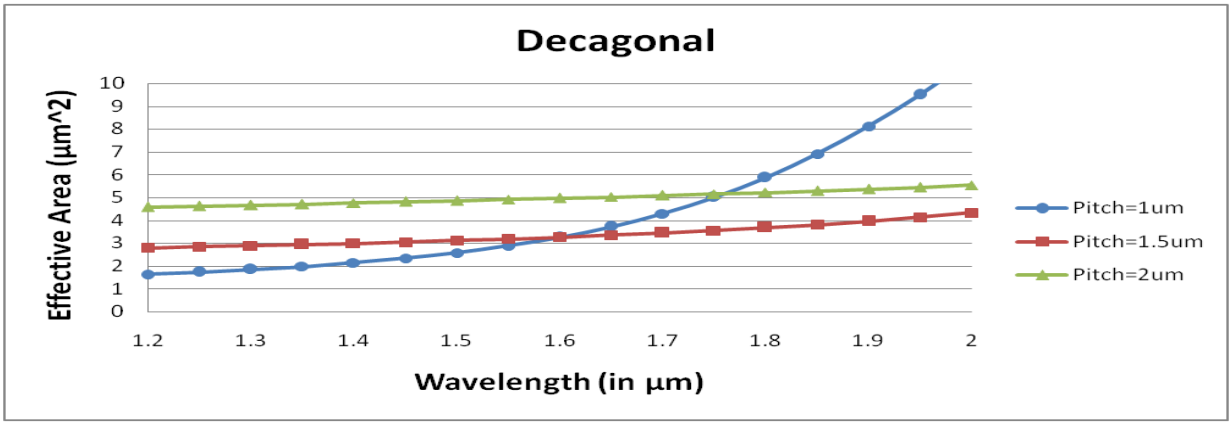

Figure 4.9: Effective Modal Area (in μm^2) v/s wavelength of Decagonal geometry with air filling fraction(d/p)=0.5 at different pitch sizes=1µm, 1.5µm, 2µm

It is observed in Figure 4.7, 4.8 and 4.9 that as the wavelength increases the Effective mode area increases and as the pitch size reduces the effective mode area reduces. At higher frequencies, the structure with pitch size 1µm losses its confinement ultimately Effective mode area suddenly increases. So overall, a structure with pitch size 1.5µm shows better confinement in all three geometries.

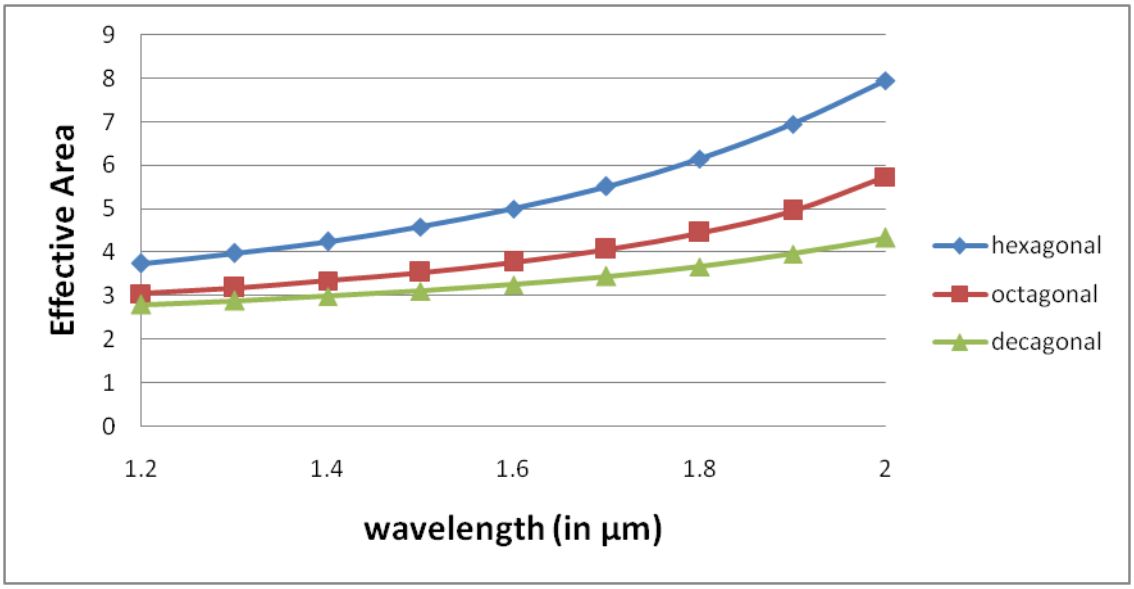

Figure 4.10: Comparative plot of Effective Modal Area (in μm^2) v/s wavelength of all three geometries with air filling fraction(d/p)=0.5 at different pitch length of 1.5µm

The graph in Figure 4.10 shows the Effective mode area for three geometries for pitch size 1.5µm and d/p=0.5. As the geometry moves to higher order polygon the effective mode area decreases, therefore confinement increases and nonlinearity also increases. Hence, decagonal geometry has a better confinement and high nonlinearity.

Table 4.3: This table shows effective mode areas (in μm^2) for different geometries at different pitch size for operating wavelength of 1.55µm.

	Hexagonal (in µm²)	Octagonal (in µm²)	Decagonal (in µm²)
p=1µm	5.98	3.99	2.88
p=1.5µm	4.79	3.65	3.183
p=2µm	6.52	5.34	4.90

It has been concluded that as the geometry shifted to higher order polygon or by increasing d/p ratio, the zero dispersion wavelengths will shift towards shorter wavelength. So, by further changing its parameters we can have flattened dispersion response over a wider frequency range. As the decagonal structure has a less Effective modal area at pitch length of 1.5μm, hence it has better confinement and high nonlinearity.

Chapter 5

Graded PCFs

In the last chapter, the three geometrical structures hexagonal, octagonal and decagonal of photonic crystal fiber with the same diameter of holes for all the rings in the individual structure have been studied. According to the literature, the basic optical properties of PCFs can be engineered by tweaking the geometries and its parameters. This implies any structural parameters such as d/p and hole arrangements, which affects the core size, indirectly affects the real part of the effective index. In this chapter, in order to study the effect of diameter of holes in different rings, the structures have been made graded. Here graded geometry means the diameter of holes in ring increases from innermost ring to the outermost ring. The various layouts have been designed for all the three geometries which are mentioned in Table 1 and their graphs for chromatic dispersion, effective area, and nonlinear coefficient has been plotted.

Parameters used:

- Pitch size=2 μm
- Diameter of hole to pitch ratio=0.3, 0.4, 0.5
- Operating wavelength=1.55μm
- Refractive index of material used=1.45 (Doped Silica)
- Number of rings of air holes=5

The screenshot of the design Layouts of all the three geometries on COMSOL Multiphysics software is represented figure 5.1.

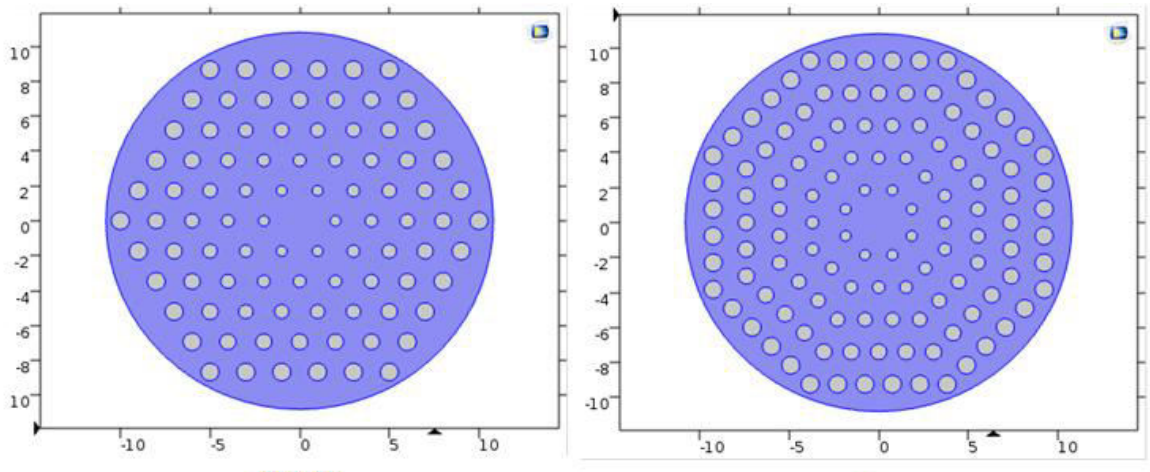

HPCF OPCF

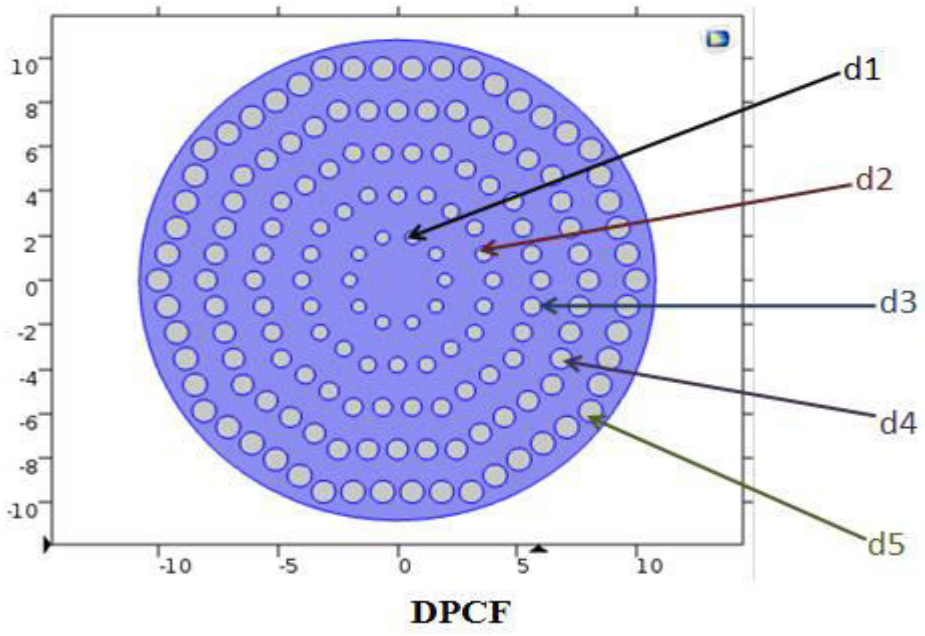

Figure 5.1: The screenshot of (a) HPCF, (b) OPCF and (c) DPCF geometries

The diameter of holes from the inner ring to outer ring is represented as d1, d2, d3, d4 and d5. The four layouts have been compared with basic structures from chapter 4. Here, d1, d2, d3, d4 and d5 are the diameters of holes (in μm) in the respective rings of the structures

Table 5.1: Summary of Layouts

	d1(hole diameter inthefirst ring in μm)	d2(hole diameter in thesecond ring in μm)	d3(hole diameter inthethird ring in μm)	d4(hole diameter in thefourth ring in μm)	d5(hole diameter inthefifth ring in μm)
Layout 1	0.3	0.3	0.3	0.3	0.3
Layout 2	0.3	0.3	0.3	0.3	0.5
Layout 3	0.3	0.3	0.3	0.5	0.5
Layout 4	0.3	0.3	0.5	0.5	0.5
Layout 5	0.3	0.5	0.5	0.5	0.5
Layout 6	0.5	0.5	0.5	0.5	0.5
Layout 7	0.2	0.3	0.4	0.5	0.5
Layout 8	0.2	0.25	0.3	0.4	0.5

5.1 Chromatic dispersion

The three different plots have been plotted for comparison of chromatic dispersion of different Layouts that are mentioned in Table 5.1

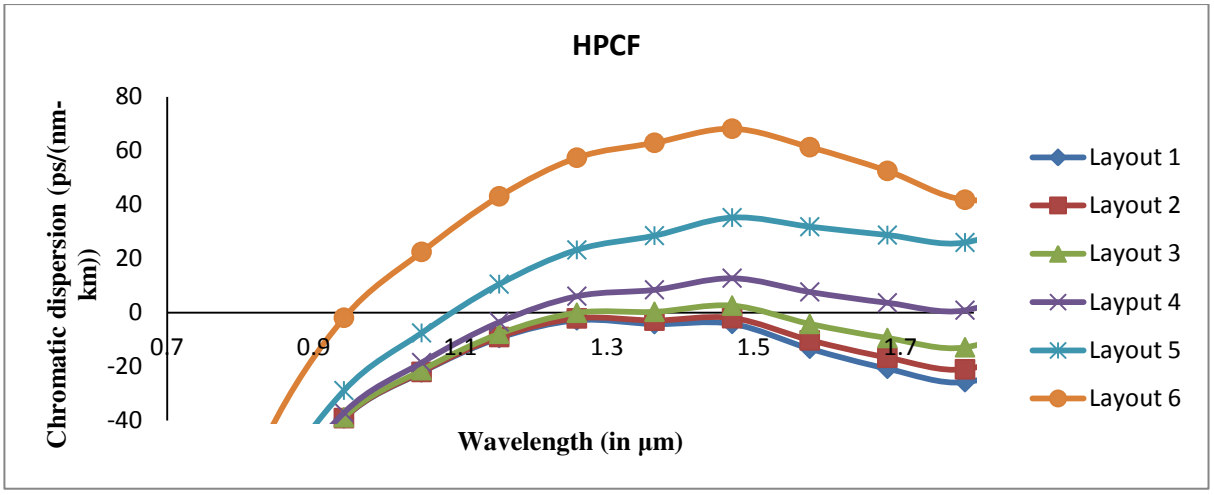

Figure5.2: Chromatic dispersion v/s wavelength graph at pitch length=2µm for different layouts of Hexagonal PCF

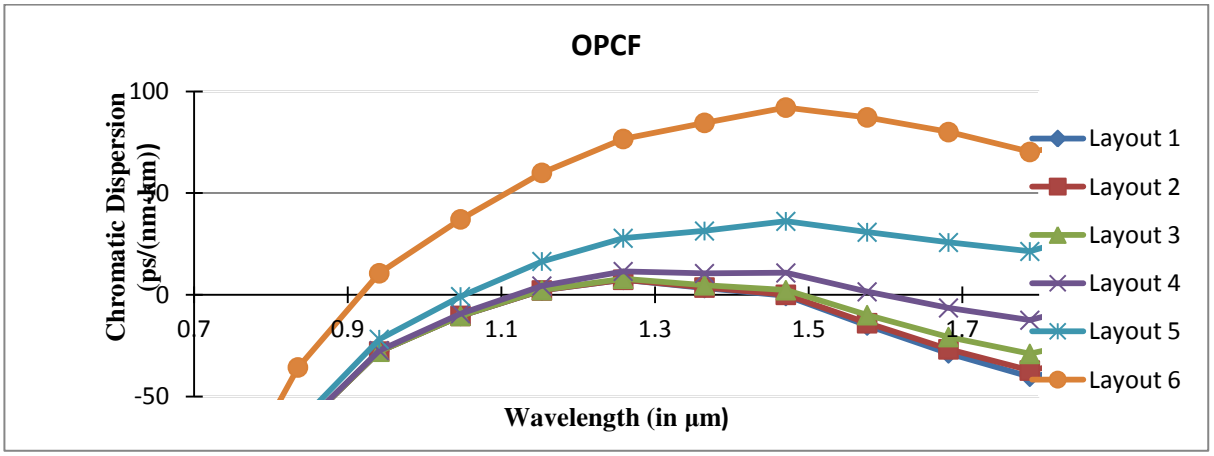

Figure 5.3: Chromatic dispersion v/s wavelength graph at pitch length=2µm for different layouts of Octagonal PCF

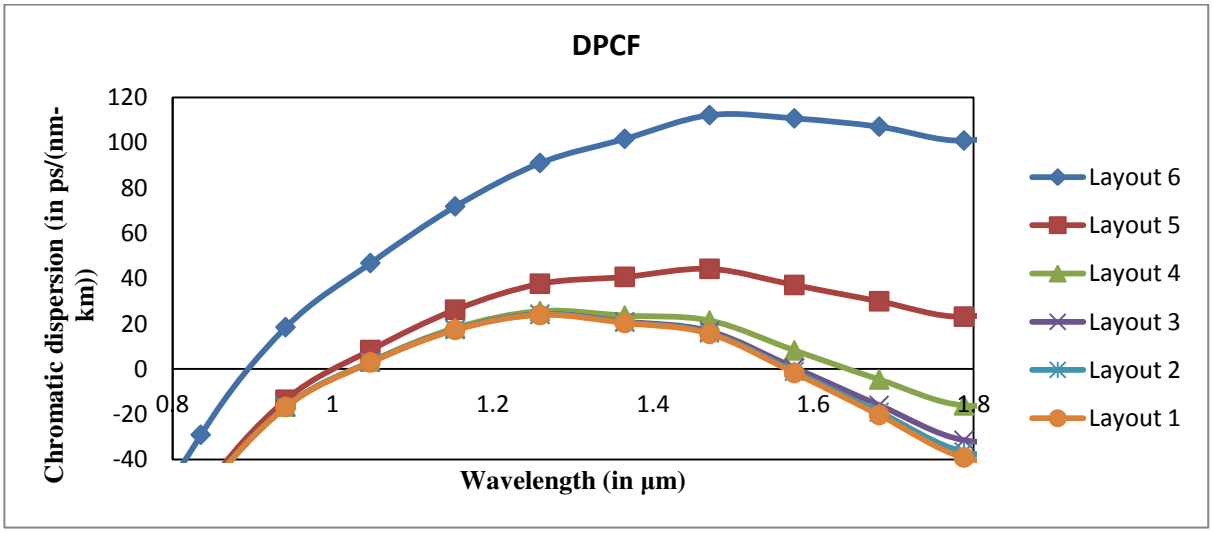

Figure 5.4: Chromatic dispersion v/s wavelength graph at pitch length=2µm for different layouts of Decagonal PCF

As the number of rings having larger diameter increases in a particular layout, the chromatic dispersion increases. So as we move from layout 1 to layout 6, the chromatic dispersion increases.

In each case, the particular layout gives flattened dispersion for a range of frequencies. The HPCF shows a dispersion variation of ±0.90839 ps/(nm-km) for the frequency range of 1.25 µm to 1.5 µm for its layout no 2. Similarly, OPCF and DPCF shows a dispersion variation of ±0.72710 ps/(nm-km) and ±4.18639 ps/(nm-km) respectively for the frequency range of 1.25 µm to 1.47µm for its layout 4. This shows the chromatic dispersion for these structures can be made flattened by further varying its ring's diameter.

Further, two more layouts have been designed which are more graded as compared to earlier structures. Here, d1, d2, d3, d4 and d5 are the diameters of holes (in µm) in the respective rings of the structures

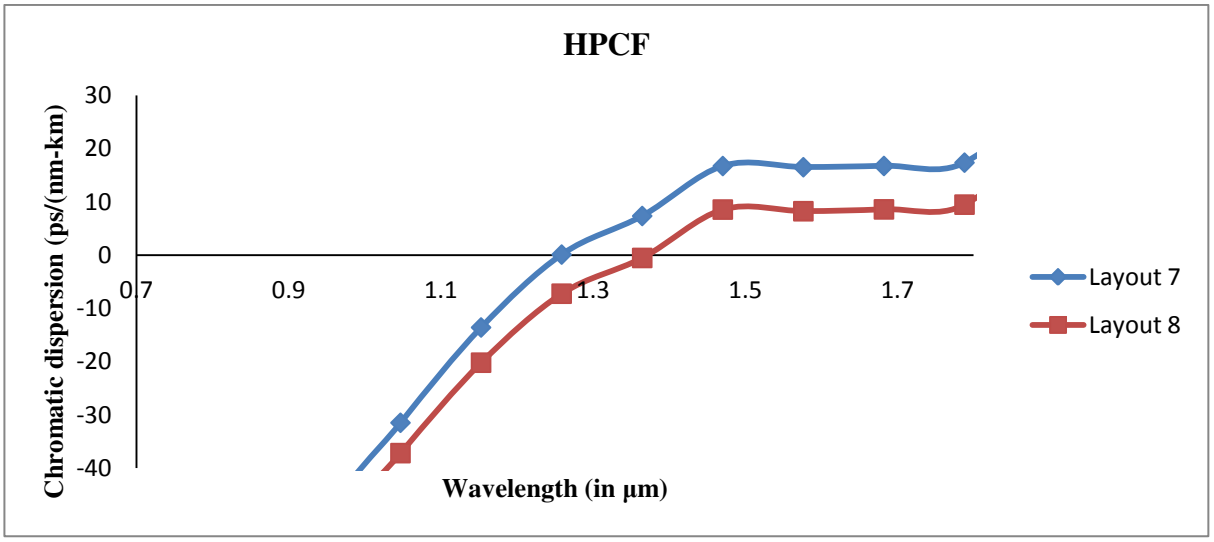

Figure 5.5: Chromatic dispersion v/s wavelength graph at pitch length=2µm for layouts 7 and 8 of Hexagonal PCF

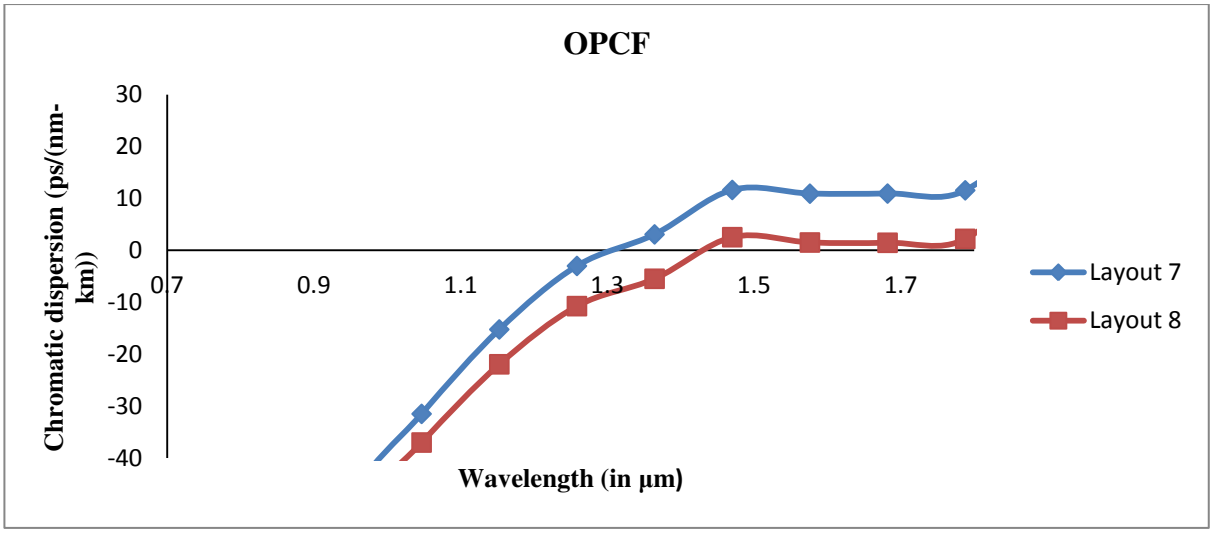

Figure5.6: Chromatic dispersion v/s wavelength graph at pitch length=2µm for layouts 7 and 8 of Octagonal PCF

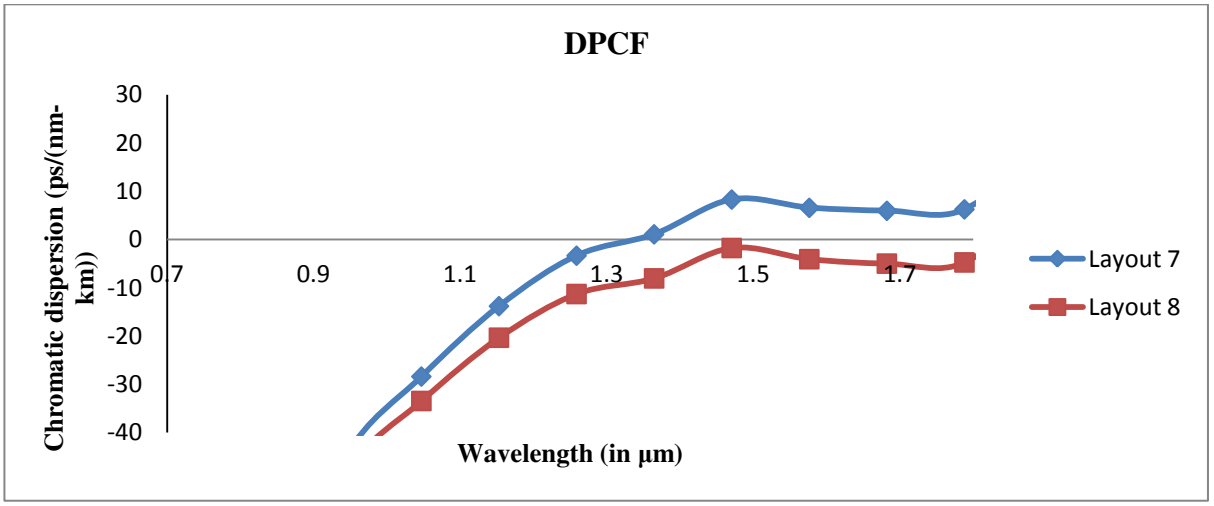

Figure5.7: Chromatic dispersion v/s wavelength graph at pitch length=2µm for layouts 7 and 8 of Decagonal PCF

All the three plots in figure 5.5, 5.6 and 5.7 represent that the Chromatic dispersion of Layout 8 in less than Layout 7 because Layout 8 is more graded with a smaller step size of the increase in diameter of air hole from the inner ring to outer ring. Also, the chromatic dispersion shown by Layout 7 and 8 are more flattened as compared to that of Layout 1 to 6. This shows that as the geometry becomes more graded the flatness in chromatic dispersion increases.

Table 5.2: The results of chromatic dispersion of layouts in Table 5.1are summarized below.

Chromatic Dispersion (in ps/(nm-km))						
	HPCF		OPCF		DPCF	
Wavelength (in μm)	Layout 7	Layout 8	Layout 7	Layout 8	Layout 7	Layout 8
0.623529412	-303.6901	-305.4759	-299.3149	-300.6020	-294.4843	-295.3163
0.729411765	-154.8481	-157.4749	-150.9011	-152.9799	-145.6256	-147.1123
0.835294118	-90.1425	-93.7589	-87.1572	-90.2527	-81.9870	-84.4145
0.941176471	-51.4468	-56.1167	-49.8525	-54.1286	-45.4217	-49.0649
1.047058824	-31.4694	-37.1664	-31.5011	-37.0197	-28.3748	-33.4311
1.152941176	-13.5762	-20.1885	-15.2455	-21.9518	-13.7891	-20.3250
1.258823529	0.1113	-7.2396	-3.0176	-10.7555	-3.3382	-11.2724
1.364705882	7.3499	-0.5256	3.0586	-5.4869	1.0895	-8.0361
1.470588235	16.7333	8.5582	11.6208	2.5218	8.2924	-1.7402
1.576470588	16.5062	8.2468	10.8997	1.4992	6.5735	-4.0570
1.682352941	16.7438	8.5919	10.9226	1.4495	5.9580	-4.9767
1.788235294	17.3665	9.4836	11.5481	2.1985	6.2570	-4.7248
1.894117647	32.3360	24.6333	26.5365	17.2521	21.0663	10.0244

In Table 5.2 colored cells show the flat range of dispersion for particular layouts of the PCF. For each structure in Layout 8 shows less dispersion as compared to Layout 7 and overall least dispersion is shown by Octagonal PCF with Dispersion variation of ±0.0497 ps/(nm-km) for the range of 1.57 μm to 1.68 μm and dispersion variation of ±1.0723 ps/(nm-km) for the range of 1.47 μm to 1.78 μm. It shows that the chromatic dispersion becomes more flattened as the structure becomes more graded.

5.2 Effective Area

The effective mode area has been calculated for the Layouts 1 to 6 of all the three geometries at different wavelengths.

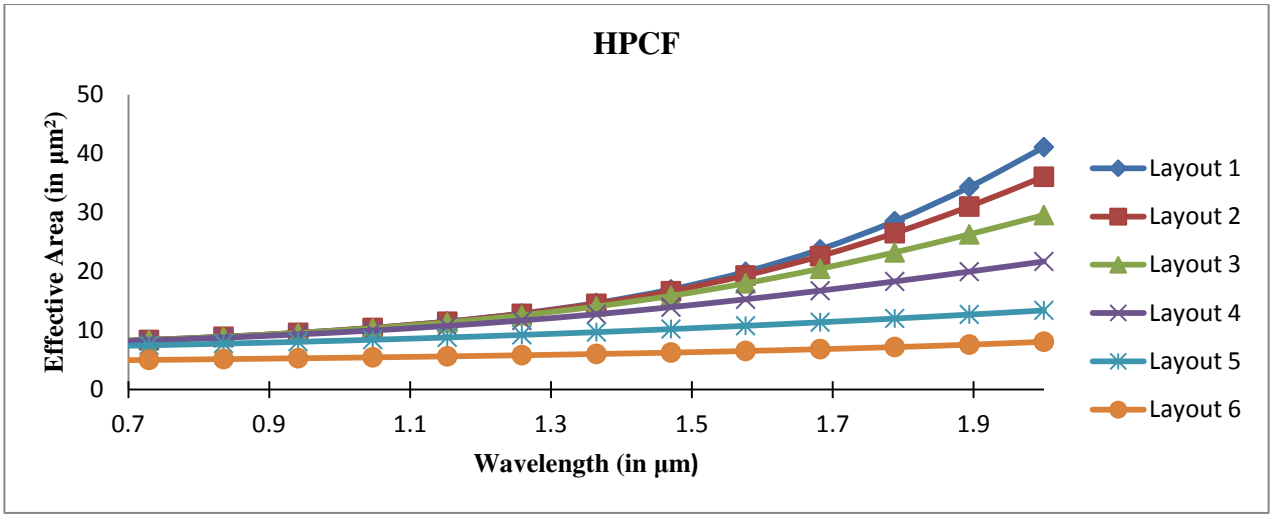

Figure 5.8: Effective Modal Area (in μm^2) v/s wavelength of hexagonal geometry for different Layouts at pitch sizes=2µm

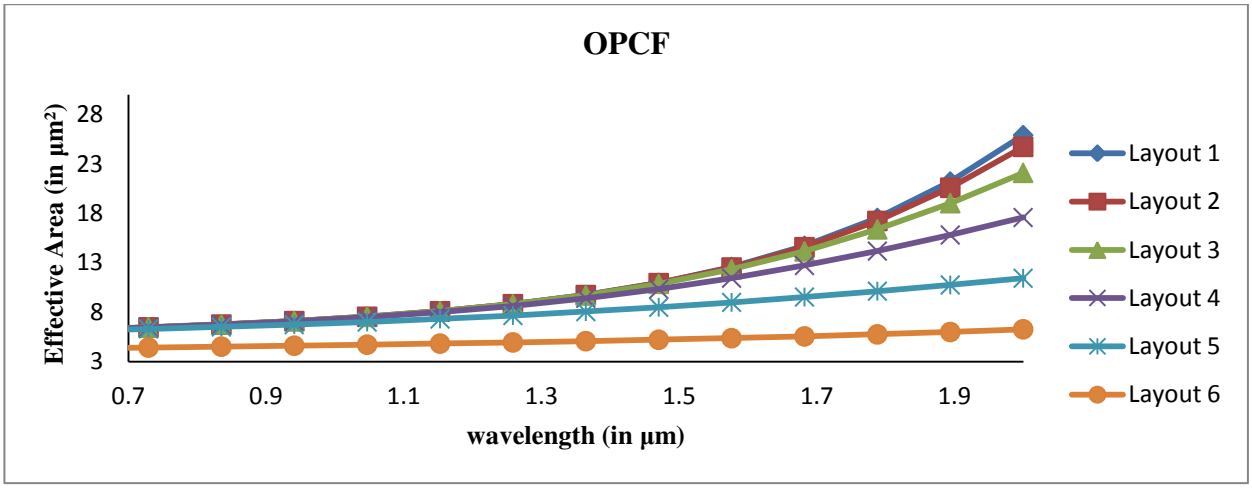

Figure 5.9: Effective Modal Area (in μm^2) v/s wavelength of octagonal geometry for different Layouts at pitch sizes=2µm

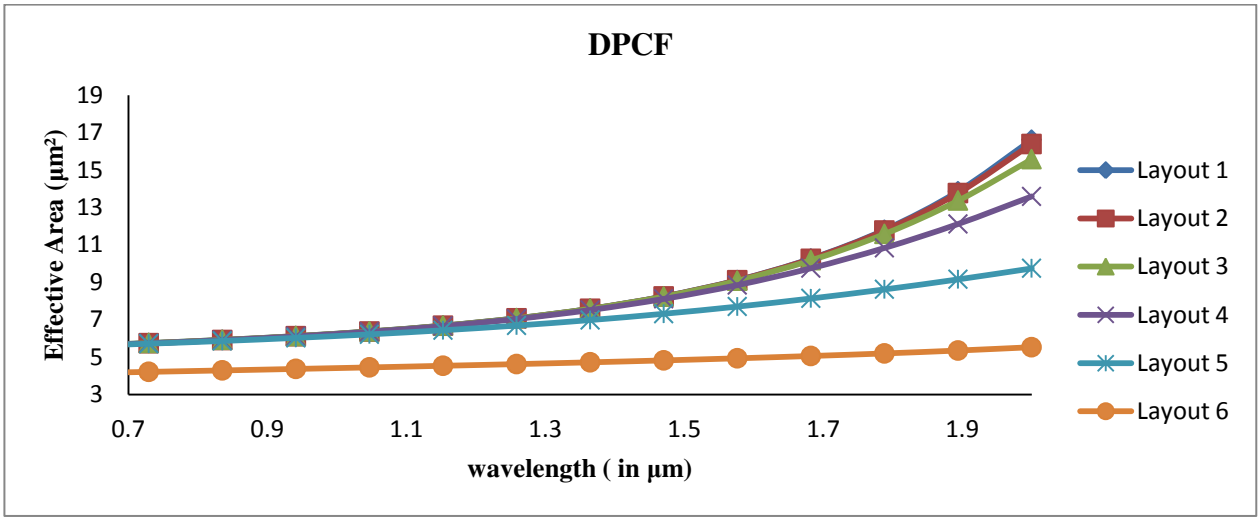

Figure 5.10: Effective Modal Area (in µm²) v/s wavelength of Decagonal geometry for different Layouts at pitch sizes=2µm

The graphs in figure 5.8, 5.9 and 5.10represent that as the wavelength increases the Effective mode area increases and as the hole diameter of inner rings decreases the effective mode area reduces. The Layout 6 shows minimum effective mode area, this means maximum confinement.

Table 5.3: The Table represents Effective Mode Area (in μm²) of different Layouts for all three geometries at operating wavelength of 1.55 μm.

	HPCF (Effective mode area in μm²)	OPCF (Effective mode area in μm²)	DPCF (Effective mode area in μm²)
Layout 1	19.95	12.56	9.11
Layout 2	19.33	12.51	9.10
Layout 3	18.00	12.32	9.08
Layout 4	15.28	11.43	8.84
Layout 5	10.81	8.98	7.70
Layout 6	6.54	5.36	4.93

It has been demonstrated that as the design becomes more graded, the chromatic dispersion curve becomes flatter for wider wavelength range. As the size of the air holes in inner rings decreases, the zero dispersion wavelengths get shifted toward higher wavelength. Also, as the size of the holes in innermost ring increases, the confinement increases and therefore effective area decreases. This shows that it is very difficult for any PCF to excel in all these properties. Some properties will have to compromise in order to maximize others. Here, the layouts with less Chromatic dispersion show greater effective mode area.

Chapter 6

PCF with Elliptical air holes

The highly birefringent fibers are used for applications like fiber optic sensing and coherent optical communications. The asymmetric microstructure design around the fiber core may lead to achieve higher birefringence. So, In order to achieve asymmetric core, the shape of the air holes around its core has been changed from circular to elliptical.

So, in this chapter, the various designs have been designed and the characteristics like chromatic dispersion, birefringence, effective area and nonlinearity coefficient have been plotted.

Parameters used:

- Pitch size=2 μm
- Diameter of hole to pitch ratio=0.4, 0.5
- Operating wavelength=1.55μm
- Refractive index of material used=1.45 (Doped Silica)
- Number of rings of air holes=5

The four different layouts have been designed with two different hole sizes with different ellipticity ratio for the ellipse. Here, the area of the circular hole and ellipse are taken same.

Table 6.1: Summary of Layouts, d1, d2, d3, d4, d5 are the diameter of the circular holes in the ring 1,2,3,4 and 5 respectively. Here, a and b represents the major axis and minor axis respectively of the ellipse.

	d1(in μm)	d2(in μm)	d3(in μm)	d4(in μm)	d5(in μm)	a(in μm)	b(in μm)
Layout 1	0.4	0.4	0.4	0.4	0.4	0.32	0.5
Layout 2	0.4	0.4	0.4	0.4	0.4	0.267	0.6
Layout 3	0.5	0.5	0.5	0.5	0.5	0.4	0.625
Layout 4	0.5	0.5	0.5	0.5	0.5	0.334	0.75

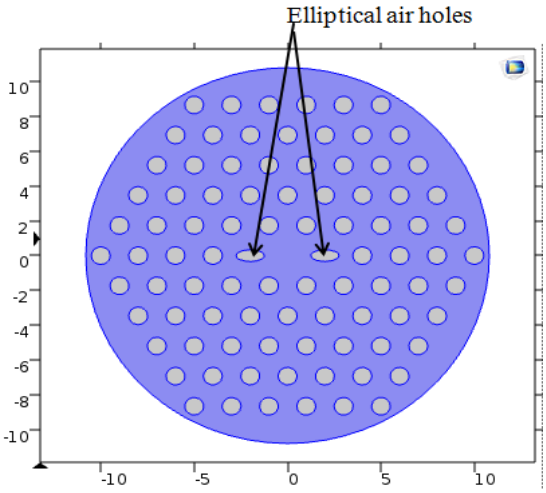

Figure6.1:Screenshot of Hexagonal geometry having elliptical air hole designed on COMSOL Multiphysics.

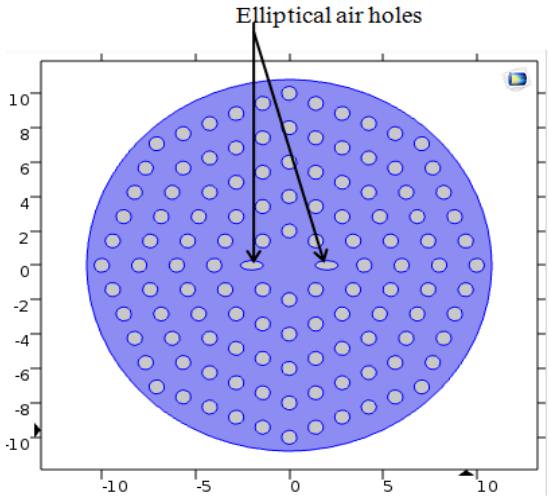

Figure 6.2: Screenshot of octagonal geometry having elliptical air hole on COMSOL Multiphysics

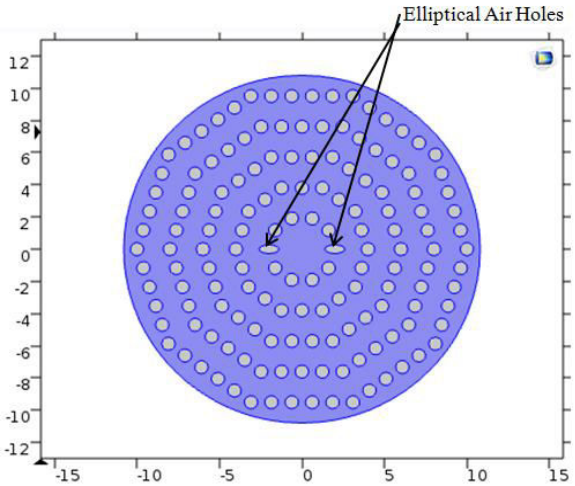

Figure 6.3: Screenshot of Decagonal geometry having elliptical air hole on COMSOL Multiphysics

6.1 Chromatic dispersion

The comparison of chromatic dispersion has been done for four layouts of all the three geometries.

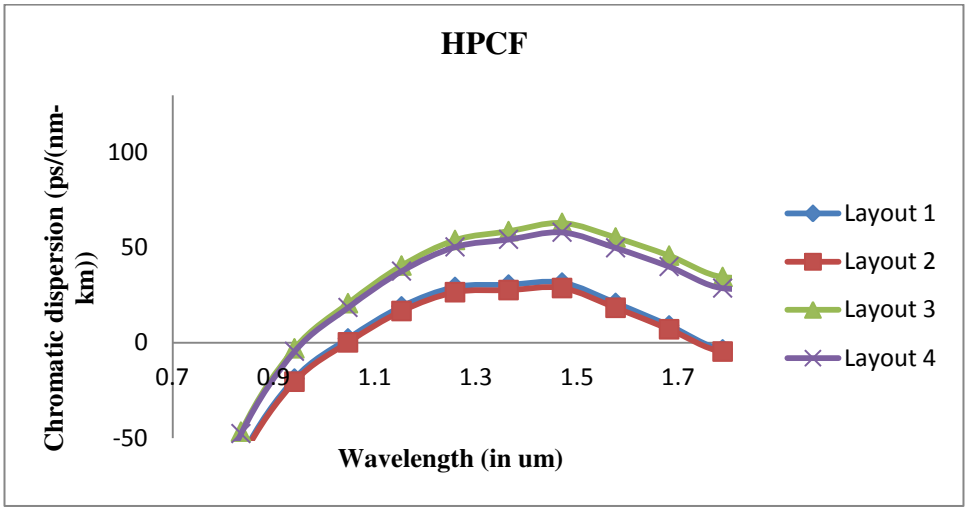

Figure 6.4: Variation of Chromatic dispersion with wavelength for different layouts of Hexagonal Geometry at operating wavelength of 1.55µm

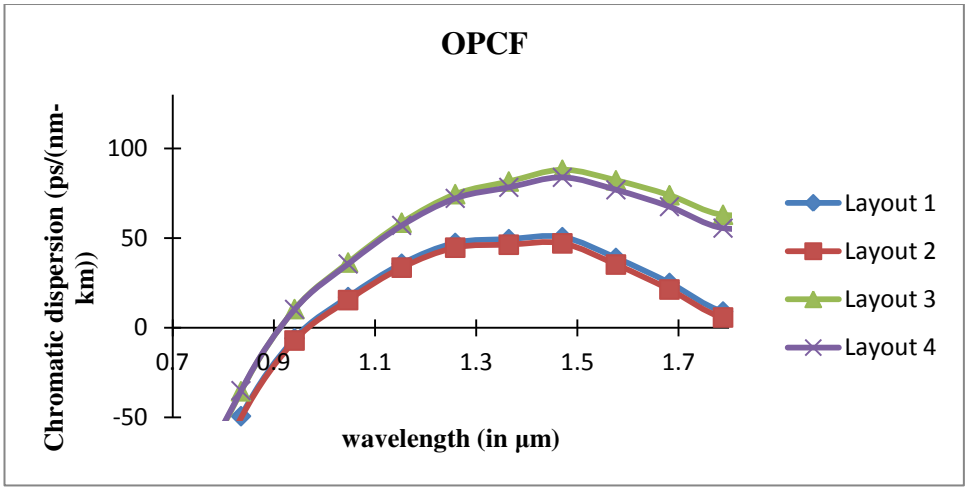

Figure 6.5: Variation of Chromatic dispersion with wavelength for different layouts of Octagonal Geometry at operating wavelength of 1.55µm

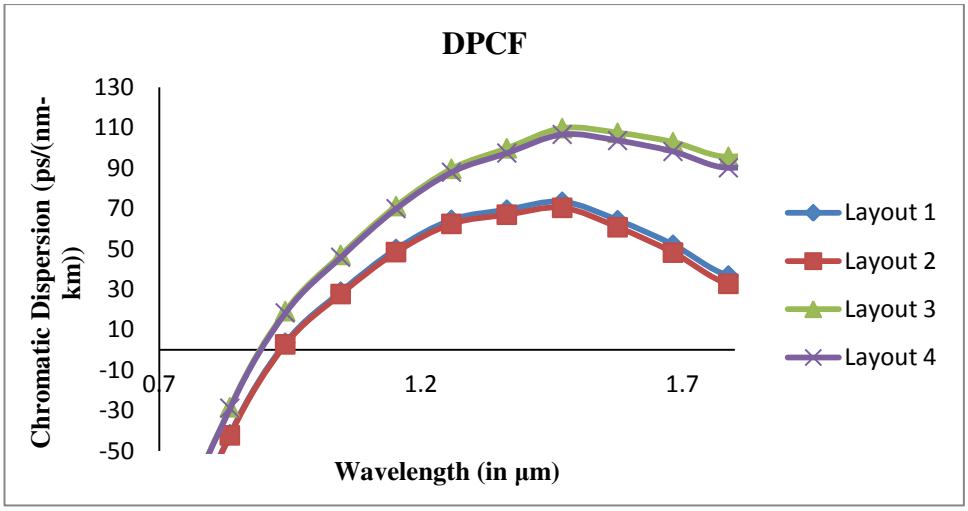

Figure 6.6: Variation of Chromatic dispersion with wavelength for different layouts of Decagonal geometry at operating wavelength of 1.55µm

The graphs have shown in Figure 6.4, 6.5and 6.6 compares the chromatic dispersion of different layouts for all three geometries hexagonal, octagonal and decagonal. As the diameter of holes increases the Chromatic dispersion increases, the layout 1 and layout 2 is showing lower chromatic dispersion than layout 3 and 4. Also as the ellipticity of holes increases the chromatic dispersion further decreases, the layout 2 and layout 4 are showing lower chromatic dispersion than layout 1 and layout 3 respectively. There is no effect on zero dispersion wavelengths for its ellipticity. The value of chromatic dispersion at operating wavelength (1.55µm)is summarized in the table 6.2.

Table 6.2: The summary of chromatic dispersion at operating wavelength of 1.55µm for designed Layouts

	Layout 1 (ps/(nm-km))	Layout 2 (ps/(nm-km))	Layout 3 (ps/(nm-km))	Layout 4 (ps/(nm-km))
HPCF	20.88	18.31	55.24	49.79
OPCF	38.89	35.20	82.17	76.87
DPCF	64.24	60.75	107.51	103.68

6.2 Birefringence

The variation of birefringence with wavelength has been calculated and represented in Figure 6.7, 6.8 and 6.9. The graphs show the value of birefringence increases with

increase in wavelength. As the diameter of air holes decreases the birefringence increases, the layout 1 has higher birefringence than layout 3, similarly, layout 2 has higher birefringence than layout 4. Also as ellipticity increases the birefringence increases.

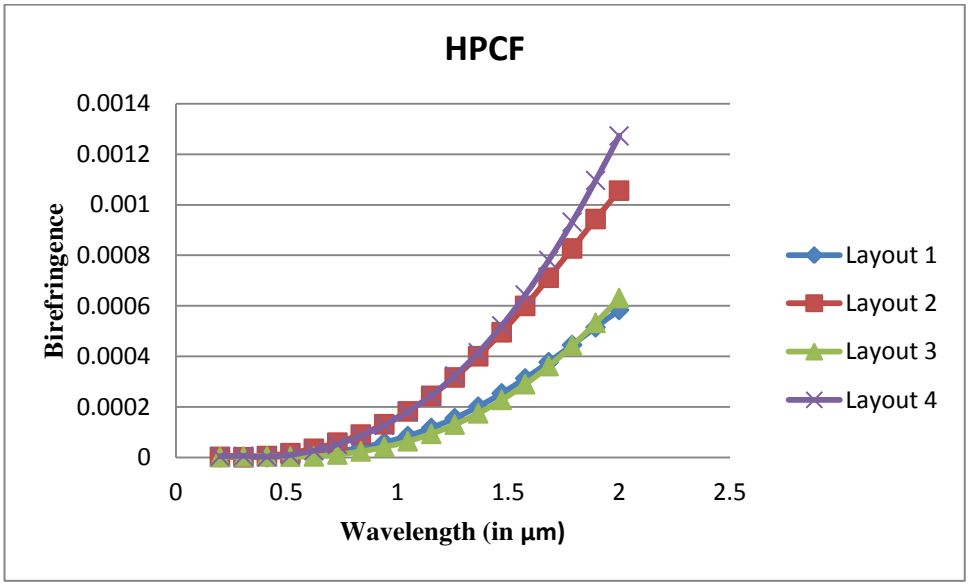

Figure 6.7: Variation of birefringence with wavelength for different Layouts of Hexagonal Geometry at operating wavelength of 1.55µm

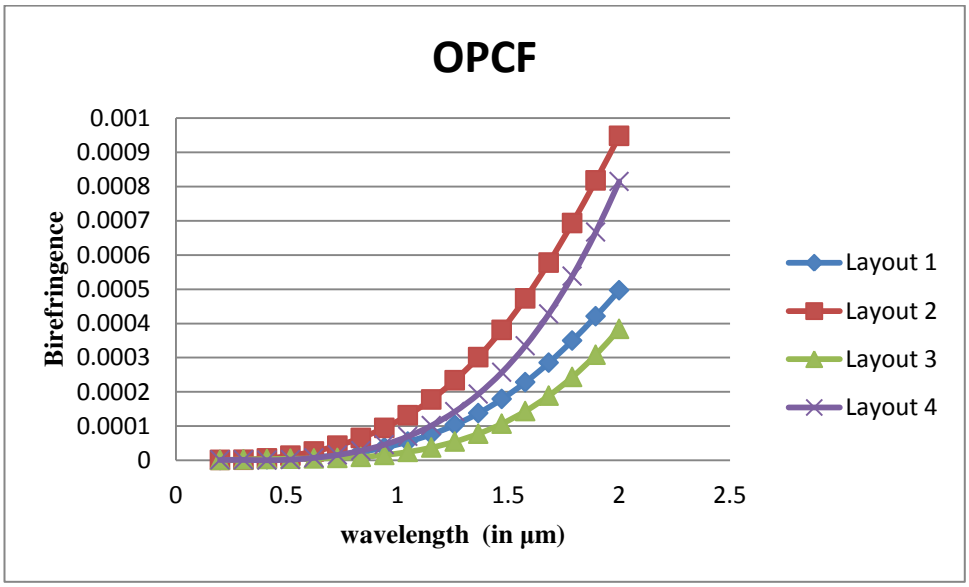

Figure 6.8: Variation of birefringence with wavelength for different Layouts of Octagonal Geometry at operating wavelength of 1.55µm

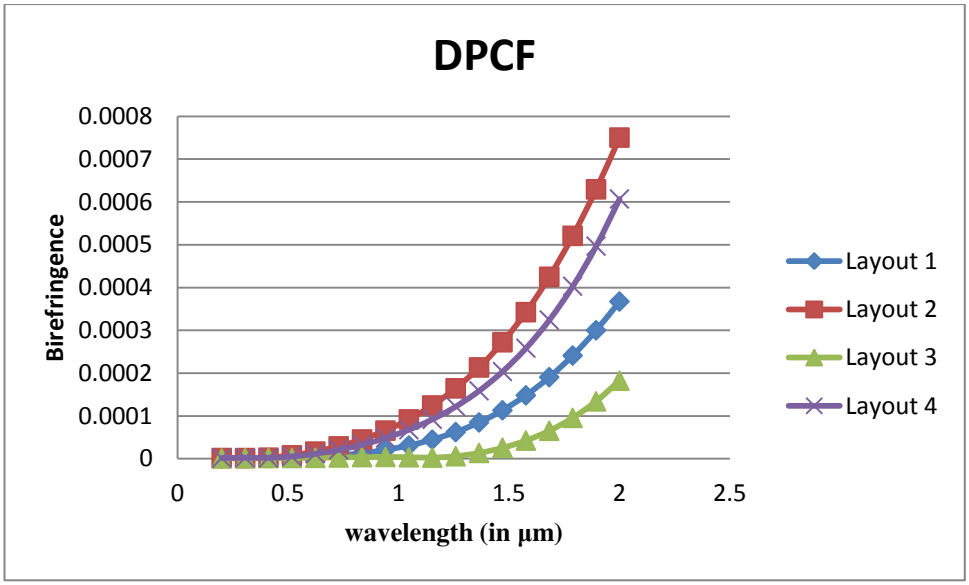

Figure 6.9: Variation of birefringence with wavelength for different Layouts of Decagonal geometry at operating wavelength of 1.55µm

Table 6.3: The summary of birefringence at operating wavelength of 1.55µm for the designed Layouts

	HPCF	OPCF	DPCF
Layout 1	0.31×10^{-3}	0.228×10^{-3}	0.148×10^{-3}
Layout 2	0.59×10^{-3}	0.473×10^{-3}	0.342×10^{-3}
Layout 3	0.29×10^{-3}	0.144×10^{-3}	0.0425×10^{-3}
Layout 4	0.64×10^{-3}	0.335×10^{-3}	0.258×10^{-3}

It has been demonstrated that as the diameter of holes decreases the chromatic dispersion decreases and birefringence increases and as the ellipticity of air holes increases the chromatic dispersion again decreases and birefringence increases at operating wavelength of 1.55 µm. There is no effect of ellipticity on zero dispersion wavelengths.

Conclusion

As the geometry shifted to higher polygon structure i.e. from hexagonal to decagonal, the zero dispersion wavelength will shift toward smaller wavelength and the chromatic dispersion at operating wavelength increases, the effective mode area decreases and thus the value of nonlinearity coefficient increases.

As the diameter to pitch ratio of the air holes in a particular geometry increases, the zero dispersion wavelengths will shift toward smaller wavelength and the chromatic dispersion increases.

As the pitch size of a particular geometry decreases, the effective mode area will decrease and thus the value of nonlinear coefficient increases.

As the design becomes more graded (diameter of air holes increases from inner ring to outer ring of structure), the chromatic dispersion curve becomes flattered forawider range of wavelength. The increased radius of air holes of the inner ring will decrease the effective mode areaand ultimately increases the value of its nonlinearity coefficient.

As the diameter of air holes decreases the birefringence increases and as the ellipticity of air holes increases again birefringence increases at operating wavelength of 1.55 μm. There is no effect of ellipticity on zero dispersion wavelengths.

Future work

The work concluded in this thesis has identified several parameters for future investigation. As demonstrated in chapter 5 and 6, the combination of the graded structure of a particular geometry with the asymmetrical core structure can leads to PCF with flat chromatic dispersion and high birefringence. This property further can be used for making various types of PCF based sensors. The design principles presented in this work will be of great value for the optimization of PCF parameters to achieve excellent optical properties.

References

[1] Rashid, M. M., Anower, M. S., Hasan, M. I., &Hasan, M. R. (2016, September). "Highly birefringent octagonal shaped photonic crystal fiber with two zero dispersion wavelengths in Ti: Sapphire oscillator range". In *Electrical Engineering and Information Communication Technology (ICEEICT), 2016 3rd International Conference on* (pp. 1-6). IEEE.

[2] Talukder, R. H., &Mou, J. R. (2016, May). "Highly birefringent squeezed hexagonal photonic crystal fiber with low nonlinear coefficient and low confinement loss". In *Informatics, Electronics and Vision (ICIEV), 2016 5th International Conference on* (pp. 83-87). IEEE.

[3] Amin, M. N., Faisal, M., &Rahman, M. M. (2016, November). "Ultrahigh birefringent index guiding photonic crystal fibers". In *Region 10 Conference (TENCON), 2016 IEEE* (pp. 2722-2725). IEEE.

[4] Ayyanar, N., Vigneswaran, D., Sharma, M., Sumathi, M., Rajan, M. M., &Konar, S. (2017). "Hydrostatic Pressure Sensor Using High Birefringence Photonic Crystal Fibers". *IEEE Sensors Journal*, *17*(3), 650-656.

[5] Kayser, S. F., Roy, S., &Khatun, M. T. (2016, December). "Design of a highly nonlinear single mode hexagonal photonic crystal fiber for high negative dispersion". In *Computer and Information Technology (ICCIT), 2016 19th International Conference on* (pp. 117-121). IEEE.

[6] Akowuah, E.K., Ademgil, H. and Haxha, S. (2012) "Design and analysis of photonic crystal fibres (PCFs) for broadband applications", doi: http//dx..org/10.1109/ICASTech.2012.6381077.

[7] Krishna, G. D., Prasannan, G., Sudheer, S. K., &Pillai, V. M. (2015). "Design of Ultra-Low Loss Highly Nonlinear Dispersion Flattened Octagonal Photonic Crystal Fibers". *Optics and Photonics Journal*, *5*(12), 335.

[8] Kaijage, S. F., Namihira, Y., Begum, F., Hai, N. H., Razzak, S. M. A., Kinjo, T., &Zou, N. (2009, July). "Highly nonlinear and polarization maintaining octagonal photonic crystal fiber in 1000nm regions". In *OptoElectronics and Communications Conference, 2009. OECC 2009. 14th* (pp. 1-2). IEEE.

[9] Mortensen, N. A., Folkenberg, J. R., Nielsen, M. D., & Hansen, K. P. (2003).”Modal cutoff and the V parameter in photonic crystal fibers”. *Optics letters*, *28*(20), 1879-1881.

[10] Kaur, A., Gupta, D. P., Devra, S., & Singh, K. (2016). Photonic Crystal Fiber: Developments and Applications.

[11] Akowuah, E. K., Ademgil, H., &Haxha, S. (2012, October). ” Design and analysis of photonic crystal fibres (PCFs) for broadband applications”. In *Adaptive Science & Technology (ICAST), 2012 IEEE 4th International Conference on* (pp. 114-120). IEEE.

[12] Chen, D., Vincent Tse, M. L., & Tam, H. Y. (2010). ”Optical properties of photonic crystal fibers with a fiber core of arrays of subwavelength circular air holes: Birefringence and dispersion”. *Progress In Electromagnetics Research*, *105*, 193-212.

[13] Razzak, S. M. A., Namihira, Y., Khan, M. G., Anower, M. S., &Hai, N. H. (2006, December). ”Transmission characteristics of circular ring pcf and octagonal pcf: A comparison”.In *Electrical and Computer Engineering, 2006.ICECE'06. International Conference on* (pp. 266-269). IEEE.

[14] Zhang, S. H., Sun, J. H., Cai, H., & Zhang, X. T. (2015, August). ”Highly Birefringent Octagonal Photonic Crystal Fibers”. In *Ubiquitous Intelligence and Computing and 2015 IEEE 12th Intl Conf on Autonomic and Trusted Computing and 2015 IEEE 15th Intl Conf on Scalable Computing and Communications and Its Associated Workshops (UIC-ATC-ScalCom), 2015 IEEE 12th Intl Conf on* (pp. 1626-1630). IEEE.

[15] Zhou, W., Wu, W., & Chen, H. (2015, October). ”Study highly birefringent hybrid lattice structure photonic crystal fiber”. In *Opto-Electronics and Applied Optics (IEM OPTRONIX), 2015 2nd International Conference on* (pp. 1-4). IEEE.

[16] Lee, Y. S., Lee, C. G., & Kim, S. (2015, August). ”Double cladding photonic crystal fiber based on dual lattice structure: high birefringence and negative flat dispersion”.In *Conference on Lasers and Electro-Optics/Pacific Rim* (p. 26P_12).Optical Society of America.

[17] Islam, M. I., Khatun, M., Sen, S., Ahmed, K., &Asaduzzaman, S. (2016, December). ”Spiral photonic crystal fiber for gas sensing

application".In *Electrical and Computer Engineering (ICECE), 2016 9th International Conference on* (pp. 238-242). IEEE.

[18] Ani, A. B., & Faisal, M. (2016, December). "Ultra-flattened broadband dispersion compensating photonic crystal fiber with ultra-low confinement loss". In *Electrical and Computer Engineering (ICECE), 2016 9th International Conference on* (pp. 243-246). IEEE.

List of Publications

Conference Paper

[1] Amritveer Kaur, Julie Devi, Ritu Sharma, Varshali Sharma, Santosh Chaudhary (2017) ”Design of Octagonal and Decagonal lattice Photonic Crystal Fiber for achieving Ultra Low flattened dispersion”. International Conference on Optical & Wireless Technologies (OWT2017) 18-19th March, 2017.

[2] Julie Devi, Amritveer Kaur, Ritu Sharma, Varshali Sharma, Santosh Chaudhary (2017) “Design and Analysis of Spiral Photonic Crystal Fiber giving Ultra Flattened Dispersion for C+L+U Band”. International Conference on Optical & Wireless Technologies (OWT2017) 18-19th March, 2017.